Asian Power Electronics Journal

PERC, HK PolyU

First edition Dec 2014 Printed in Hong Kong by Reprographic Unit
The Hong Kong Polytechnic University

Published by

Power Electronics Research Centre
The Hong Kong Polytechnic University
Hung Hom, Kowloon, Hong Kong

ISSN 1995-1051

Disclaimer

Any opinions, findings, conclusions or recommendations expressed in this material/event do not reflect the views of The Hong Kong Polytechnic University

Editorial board

Table of Content

Power Transfer Capability Improvement to HVDC Transmission System using Artificial Neural Network and Inference System (ANFIS) Controller

M. Ramesh [1] A. Jaya Laxmi [2]

Abstract–High Voltage Direct Current (HVDC) Transmission systems traditionally employ PI controllers with fixed proportional (P) and integral (I) gains K_p and K_i respectively. Although such controllers are robust and simple, they are not easily optimized to obtain the best performance under all conditions. In the field of intelligent control systems, fuzzy logic control and artificial neural network based control are the two most popular control methodologies being used. Neuro-fuzzy systems, as the name suggests combine ANNs and fuzzy logic into one system. The aim of such a combination is to inherit advantages of both the intelligent control techniques and shunt out their individual disadvantages. The CIGRÉ model as one of the conventional methods has been studied and new complementary characteristics have been added to improve its stability and damping rate of voltage and current oscillations during the disturbance in the AC Systems and to increase the efficiency of the proposed model.

Keywords–HVDC transmission, CIGRÉ Benchmark model, faults in HVDC system, proportional integral (PI) Controller, ANFIS controller.

I. INTRODUCTION

High Voltage Direct Current (HVDC) Transmission is the preferred method for bulk Transmission of power over long distances [1]. HVDC System is a mature Technology [2], starting from mercury-arc to thyristors and presently to IGBT and IGCT valves, from conventional PI Controllers to more advanced Control Techniques. Further work needs to be done particularly on the Control aspects to further improve the Transmission performance and efficiency of such Systems. The performance of these systems depends on the control method being used. Furthermore, the control of a HVDC System remains a formidable challenge because of various factors such as changes in system conditions, converter Transformer saturation characteristics, presence of AC/DC filters, and the generation of harmonics by converter units which makes the HVDC System highly complex and non-linear [3]. Since fuzzy logic uses intuitive rules for the control of the system, a detailed system model is not required. This makes Fuzzy Logic well-suited for use with complex and nonlinear systems, such as HVDC Systems. Earlier research on the use of Fuzzy Logic to tune the PI Controller parameters employed constant triangular Membership functions [4]–[7]. The past work generally concluded that fuzzy logic could improve the performance of HVDC systems under various fault conditions or operating point changes, by decreasing the number of commutation failures, improving the commutation margin, or dampening oscillations.

The use of properly-designed neuro-fuzzy logic controllers has been widely shown to provide at least marginal improvement in the operation of HVDC systems compared to the use of conventional constant-parameter PI controllers [4]–[9]. This is explained by the fact that the tuning of constant-parameter PI controllers is a compromise between the speed of response and stability after small disturbances, and the robustness to tolerate large signal disturbances due to faults.

II. HVDC TEST SYSTEM

The CIGRE benchmark HVDC system model [10], used here as the test system, has been designed for conducting performance comparisons between different HVDC system control strategies. The system is shown in Fig. 1.

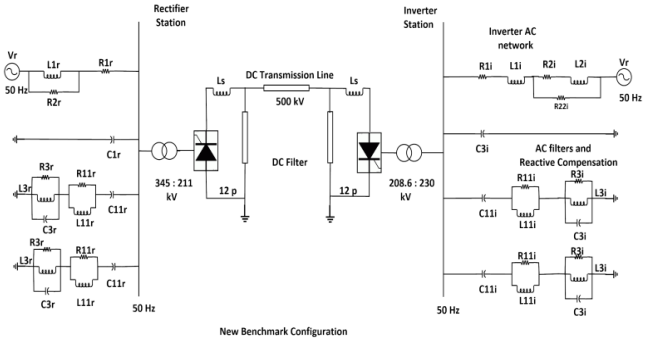

Fig. 1: Single-line diagram of the CIGRÉ benchmark HVDC system.

The short circuit ratios (SCRs) and Effective Short Circuit Ratios (ESCRs) for the CIGRE model are:

$$SCR = \frac{Short\ Circuit\ MVA\ of\ \ AC\ System}{\text{DC}\ Converter\ MW\ \ Rating}$$

(i) Rectifier: $SCR = 2.5\angle 84^{o}$

(ii) Inverter: $SCR = 2.5\angle 75^{o}$

These short circuit ratios characterize a weak system, and it is well-known that an HVDC System converter feeding into a weak AC System is prone to commutation failures. There is also a DC side resonance at near fundamental frequency and an AC-side resonance near the second harmonic frequency. Overall, the system has been specifically designed to be particularly onerous for DC control operation, and thus, it is a good choice for the test system in HVDC system control studies [8]. The control system must control a quantity such as the DC current or

The paper first received 10 June 14 and in revised form 28 Dec 2014.
Digital Ref: APEJ_2014-06-0439

[1] Associate Professor &HOD, EEE Dept, Medak College of Engineering and Technlogy, KondapakMedakDist, Research Scholar, EEE Dept., JNTU, Anantapur-515002, Andhra Pradesh, India.
E-mail: Marpuramesh223@ gmail.com

[2] Professor, Dept. of EEE & Coordinator Centre for Energy Studies, ,Jawaharlal Nehru Technological University, Hyderabad, College of Engineering, Kukatpally, Hyderabad-500085, Telangana, India. Email:ajl1994@yahoo.co.in

transmitted power, ensure stable operation in the presence of small system disturbances, and minimize the consequences of large disturbances or faults. To obtain these objectives while consuming minimum reactive power, the firing angles must be minimized [11]. The rectifier operates under constant current (CC) control to control the DC current and the inverter usually operates under constant extinction angle (CEA) control to regulate the DC voltage. For nominal conditions, the CEA control ensures the extinction angle stays at its nominal value of 150, resulting in small reactive power consumption while providing ample commutation margin to prevent commutation failures. In a two terminal HVDC System, the current margin control method is normally utilized whereby the rectifier is kept in current control (CC) and the inverter is in constant extinction angle (CEA) control. An error signal, I_e, which is the difference between the reference current, I_d, and the measured current, *Id*, from the system, is fed to the PI-controller. The error output of the controller is acted upon by the PI gains to provide the required alpha order for the HVDC converter. Due to uncertainties in system parameters, the optimal choice of gains is quite difficult. Proportional Integral (PI) controllers are commonly used in HVDC System in addition to AI controllers. A mathematical model of the real plant is required for the controller design with conventional methods. The difficulty of identifying the accurate parameters for a complex nonlinear and time-varying nature of real plants may render, in many cases, the fine tuning of parameters which is time consuming. Fig. 2 shows the structure of PI controller.

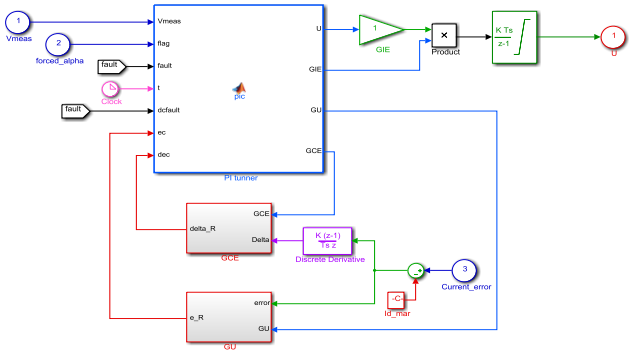

Fig. 2: Structure of PI controller.

III. Artificial Neural Network and Inference System Controller (ANFIS)

Previously, control techniques assumed a fixed mathematical model of the plant but since HVDC systems are highly uncertain, obtaining an accurate mathematical model of the plant is not possible. Consequently, a lot of research is being conducted in the application of intelligent control techniques such as fuzzy logic, neural networks and genetic algorithms to the control of HVDC systems. Fuzzy logic (FL) based controllers have been successful in improving the performance of the HVDC system [11] ,However a combination of fuzzy logic and artificial neural networks (ANNs) were used. Artificial Neural Network and Inference System

(ANFIS) is developed from sugeno-type fuzzy inference system (FIS) for effective data processing. The development is a simple data learning technique by using configuration of neuro-fuzzy model with hybrid learning rule. FIS processes a given input mapping to get a target output. This process involves membership function, fuzzy logic operators and if-then rules. It has multiple inputs and a single output with the capability in handling highly non-linear functions and predicting future value of a chaotic time series. Compared to the capabilities of the approaches such as cascaded-correlation ANN, back propagation ANN, sixth-order polynomial and other earlier methods, the result obtained from the ANFIS gives a better performance in non-dimensional error index [10]. Every stage of ANFIS shown in Fig. 3 has a particular function which is used to calculate input and output parameter sets as described below [10].

Stage 1: In the process of input fuzzification, the following equations are utilized:

$$X_i(x) = 1/[1+((x-c_i)/a_i)\text{^}2]\text{^}(b_i) \qquad i = 1,2 \tag{1}$$

$$Y_i(x) = 1/[1+((y-c_i)/a_i)\text{^}2]\text{^}(b_i) \qquad i = 1,2 \tag{2}$$

where *Xi* and *Yi* are fuzzified input values, whereas a_i, b_i and c_i are the parameter sets from the Gaussian input membership function.

Stage 2: Application of fuzzy operators involves the use of the product (AND) to the fuzzified input. (3) to (6) represent the fuzzy relations obtained from the product of fuzzy operators.

$$R1 = X1(x) \times Y1(y) \tag{3}$$

$$R2 = X1(x) \times Y2(y) \tag{4}$$

$$R3 = X2(x) \times Y1(y) \tag{5}$$

$$R4 = X2(x) \times Y2(y) \tag{6}$$

Stage 3: In the application method of rules, the activation degree and normalization is implemented by using the following equations:

$$G_i = R_i / RT \qquad i = 1,2,3,4 \tag{7}$$

where

$$RT = R1 + R2 + R3 + R4 \tag{8}$$

Stage 4: Aggregation of all outputs are obtained by using (9) which is the product of the normalized activation degree and individual output membership function,

$$O_i = G_i(pi \cdot x + gi \cdot y + ri) \qquad i = 1,2,3,4 \tag{9}$$

where *pi*, *qi* and *ri* are the parameters from the output membership function.

Stage 5: The required results are obtained through defuzzification process and it utilizes the following equation:

$$OT = \sum Oi \qquad i = 1,2,3,4 \tag{10}$$

With the advent of artificial intelligent techniques, these drawbacks can be mitigated. One such technique is the use of fuzzy logic in the design of controller either independently or in hybrid with PI controller. ANFIS replaces the draw-backs of fuzzy logic control and artificial neural network. ANFIS combines the learning power of neural network with knowledge representation of fuzzy logic. ANFIS techniques have emerged from the fusion of Artificial Neural Networks (ANN) and Fuzzy Inference Systems (FIS) and have become popular for solving the real world problems [9]. Fig. 4 shows the overall structure of Artificial Neural Network and

Inference System model. Fig. 5 shows HVDC System with ANFIS Controller.

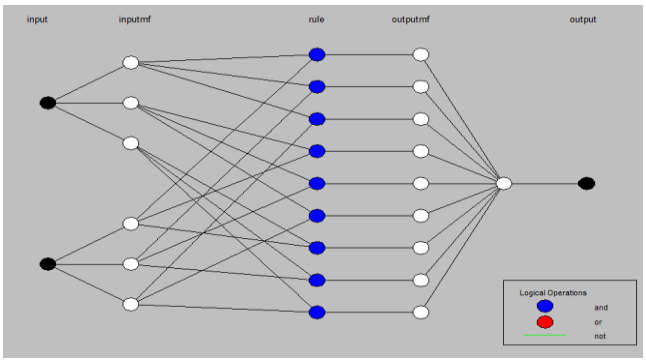

Fig. 3: Basic ANFIS structure.

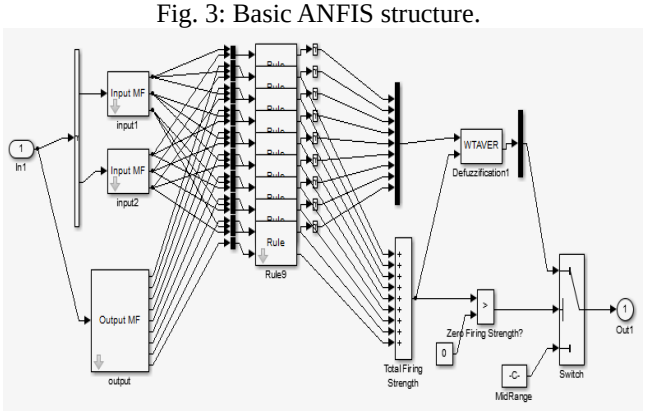

Fig. 4: Artificial Neural Network and Inference System model.

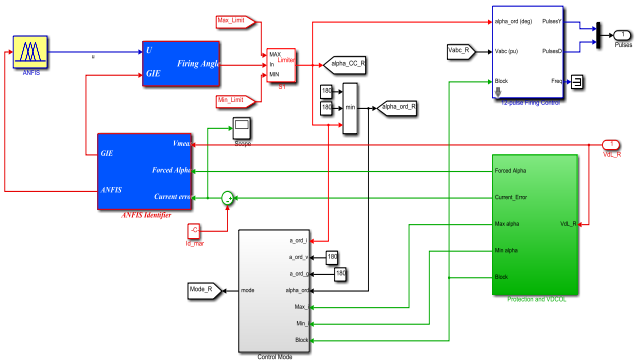

Fig. 5: HVDC system with ANFIS controller.

IV. Comparison on Performance Assessment of ANFIS Controller Based HVDC Transmission System

The rectifier and the inverter are 12-pulse converters using two universal bridge blocks connected in series. The converters are interconnected through a 850 km line and 0.597H smoothing reactors as shown in Fig. 6 the converter transformers (Wye grounded/Wye/Delta) are modeled with three-phase transformer (Three-Winding) blocks.

The HVDC Transmission link uses 12-pulse thyristor converters. Two sets of 6-pulse converters are needed for the implementation stage. The firing-angle control system is configured based on two 6-pulse converters in series, one of which is operated as a modified HVDC bridge. Here, MATLAB/SIMULINK program is used as the simulation tool. Two 6-pulse Graetz bridges are connected in series to form a 12-pulse converter. The two 6-pulse bridges are 345kV, 50 Hz totally identical except there is an in phase shift of 58.4 ° for the AC supply Voltages. Some of the harmonic effects are cancelled out with the presence of 60 ° phase shift. The harmonic reduction can be done with the help of filters. The firing angles are always maintained at almost constant or as low as possible so that the voltage control can be carried out. The control of power can be achieved by two ways i.e., by controlling the current or by controlling the Voltage. It is crucial to maintain the voltage in the DC link constant and only adjust the current to minimize the power loss. The rectifier station is responsible for current control and inverter is used to regulate the DC Voltage. Firing angle at rectifier station and extinction angle at inverter station are varied to examine the system performance and the characteristics of the HVDC System.

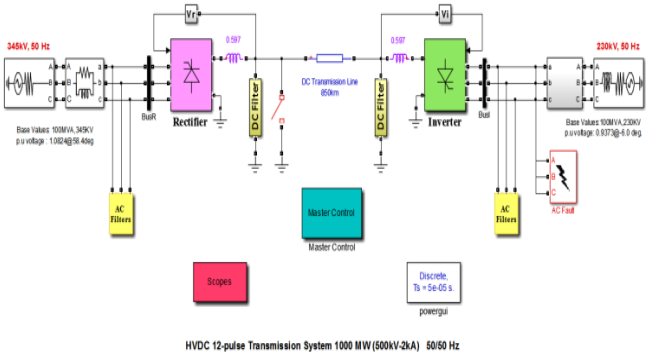

Fig. 6: Simulink diagram of the HVDC Circuit.

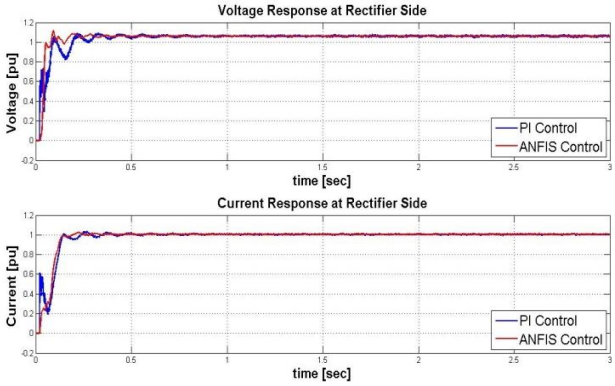

Fig. 7: Voltage and current on the DC side at rectifier (without fault).

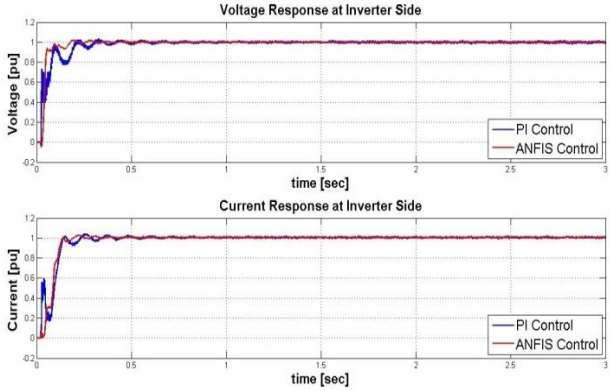

Fig. 8: Voltage and current on the DC side at inverter (without fault).

Fig. 7 and Fig. 8 show the system with no fault in voltage and current waveforms at rectifier and inverter sides using PI and the Artificial Neural Network and Inference System (ANFIS). From the simulation results it is observed that voltage and current reaches the reference value of 1.0Pu at

0.25 second, *i.e.* about 0.1 seconds later after starting HVDC System. It is clear that for no fault, both the controllers perform well but ANFIS gives a better transient performance and quite a low overshoot as compared to the conventional PI controller. The complete HVDC system reaches stable state after 0.25sec.

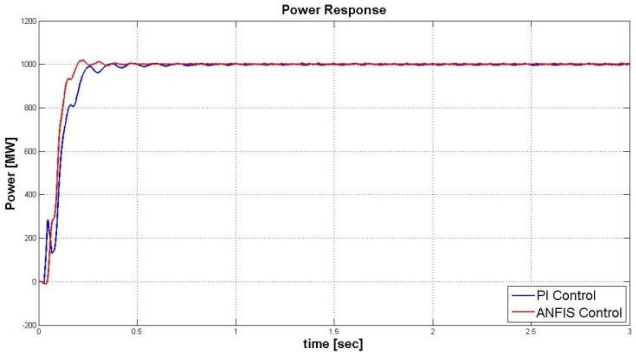

Fig. 9: Active power at rectifier.

Fig.9 shows the change process of the active power of HVDC system without fault with PI controller and the Artificial Neural Network and Inference System (ANFIS). It is clear that for no fault, both the controllers perform well but ANFIS gives a better transient performance and quite a low overshoot as compared to the conventional PI controller.

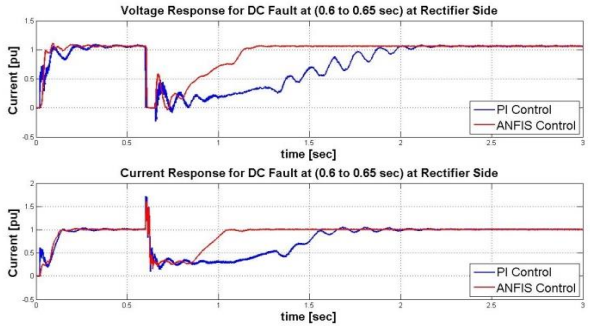

Fig. 10: When DC fault occurs on rectifier

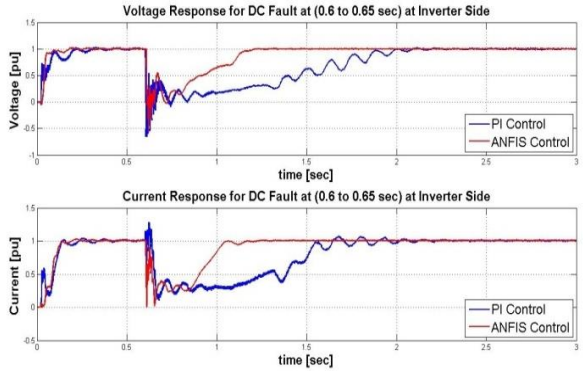

Fig. 11: When DC fault occurs on inverter

In Fig. 10 and Fig. 11, it is observed that DC fault occurs at time 0.6 sec. the fault is created for duration of 0.05 sec. at Rectifier and inverter side of HVDC System. The Artificial Neural Network and Inference System (ANFIS) activates and clears the fault. Fig. 10 and Fig. 11 show the waveforms after 0.6sec. DC fault at the rectifier and inverter. A large number of oscillations have been observed in DC link current and voltage magnitudes in case of a conventional controller. ANFIS reduces the recovery time by 1.2 sec after the disturbance. Once the fault is cleared, at t=1.2 sec the system comes back to its normal operation.

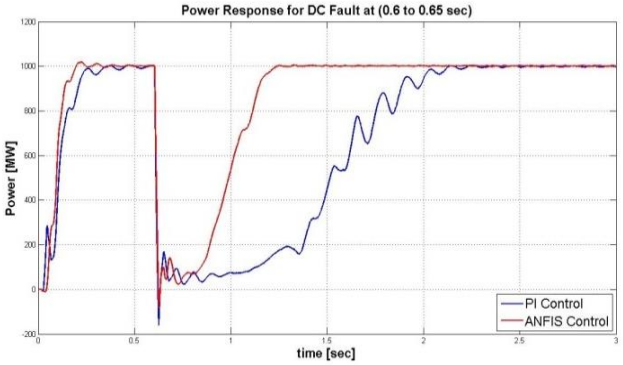

Fig. 12: Active power when DC fault occurs

Fig. 12 shows the change process of the active power of HVDC System after a disturbance of a DC fault with PI controller and Artificial Neural Network and Inference System (ANFIS). It is clear that for DC fault, both the controllers perform well but ANFIS gives a better transient performance and quite a low overshoot as compared to the conventional PI controller.

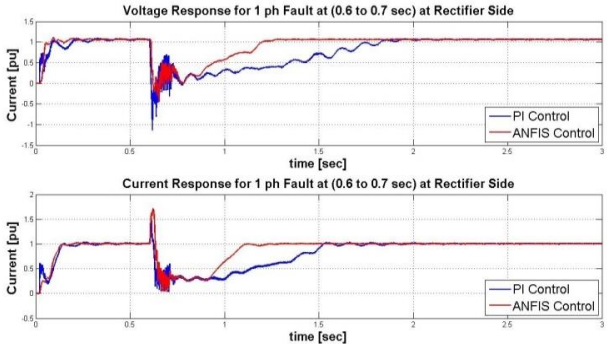

Fig. 13: When a line-to-ground fault occurs on rectifier side

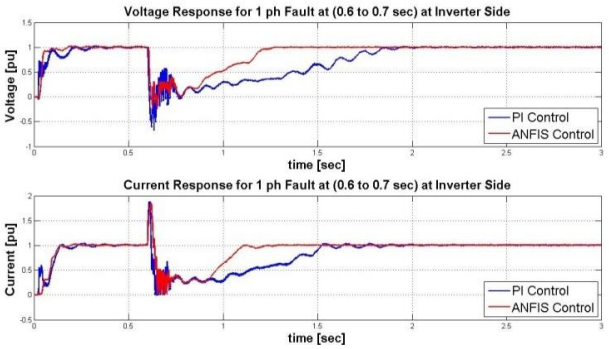

Fig. 14: When a line-to-ground fault occurs on inverter side

In Fig. 13 and Fig. 14, it is observed that a line-to-ground fault occurs at time 0.6 sec. the fault is created for duration of 0.1 sec. on phase A of the rectifier and inverter sides of HVDC System. Artificial Neural Network and Inference System (ANFIS) activates and clears the fault. ANFIS) performs better than the fixed-gain PI controller. The rectifier side DC current suffers from prolonged oscillations and consequently more commutation failures occur in the case of fixed-gain PI controller. The fixed-gain PI controller takes longer time to recover after fault is cleared due to the narrow range of optimum controller gain parameters. ANFIS reduces the recovery time by 1.2

sec after the disturbance. Once the fault is cleared, at t=1.2 sec the system comes back to its normal operation.

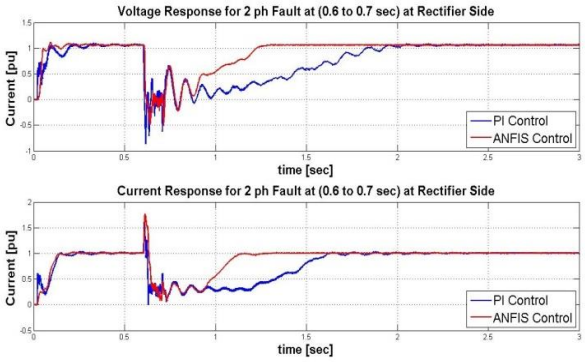

Fig. 15: When a two-phase fault occurs on rectifier side.

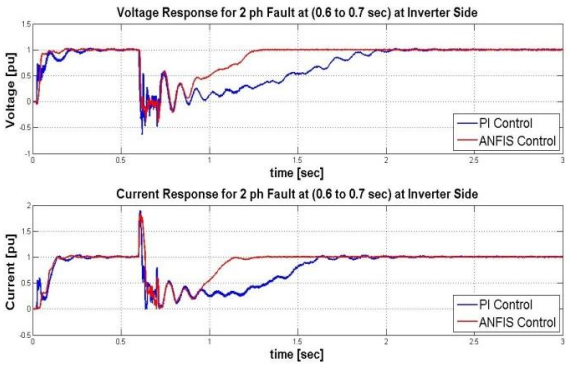

Fig. 16: When a two-phase fault occurs on inverter side.

In Fig. 15 and Fig. 16, it is observed that a two-phase fault occurs at time 0.6 sec. the fault is created for a duration of 0.1 sec. on phase A and phase B of the rectifier and inverter sides of HVDC System. Artificial Neural Network and Inference System (ANFIS) activates and clears the fault. The ANFIS performs better than the fixed-gain PI controller. The rectifier side DC current suffers from prolonged oscillations and consequently more commutation failures occur in the case of fixed-gain PI controller. The fixed-gain PI controller takes longer time to recover after fault is cleared due to the narrow range of optimum controller gain parameters. ANFIS reduces the recovery time by 1.2 sec after the disturbance. Once the fault is cleared, at t=1.2 sec the system comes back to its normal operation.

In Fig. 17 and Fig. 18, it is observed that a three-phase fault occurs at time 0.6 sec. the fault is created for a duration of 0.1 sec. on phase A and phase B of the rectifier and Inverter sides of HVDC System. Artificial Neural Network and Inference System (ANFIS) activates and clears the fault. The ANFIS performs better than the fixed-gain PI controller. The rectifier side DC current suffers from prolonged oscillations and consequently more commutation failures occur in the case of fixed-gain PI controller. The fixed-gain PI controller takes longer time to recover after fault is cleared due to the narrow range of optimum controller gain parameters. ANFIS reduces the recovery time by 1.2 sec after the disturbance. Once the fault is cleared, at t=1.2 sec the system comes back to its normal operation.

Figs.19, 20 and 21 show the change process of the active power of HVDC system after a line-to-ground fault, two-phase fault and three-phase fault are occurred with PI controller and the Artificial Neural Network and Inference System (ANFIS). It is clear that for a line-to-ground fault, two-phase fault and three-phase fault, both the controllers perform well but ANFIS gives a better transient performance and quite a low overshoot as compared to the conventional PI controller.

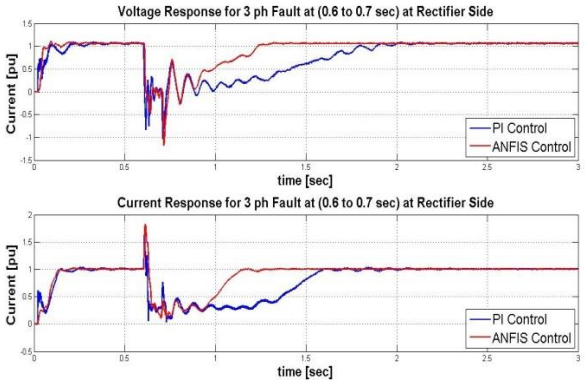

Fig. 17: When a three-phase fault occurs on rectifier side.

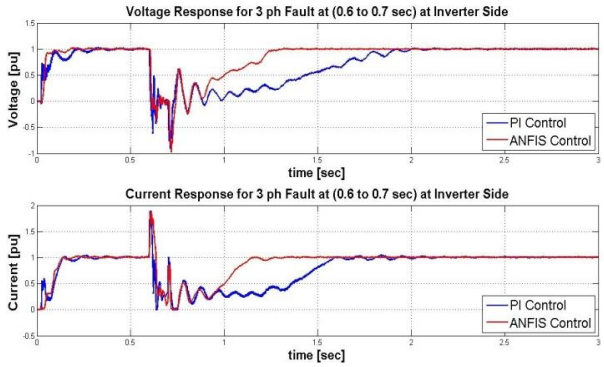

Fig. 18: When a three-phase fault occurs on Inverter side.

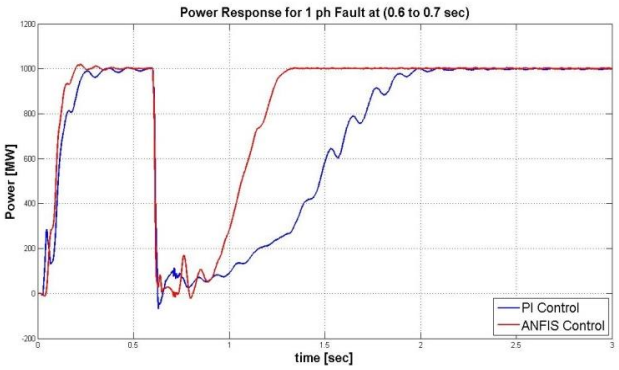

Fig. 19: Active power when a line-to-ground fault occurs.

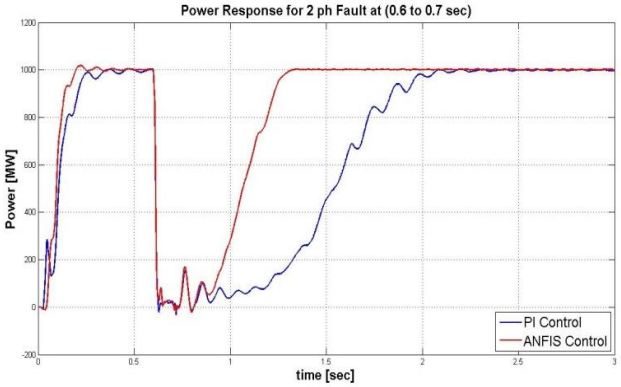

Fig. 20: Active power when a two-phase fault occurs.

Fig. 21: Active power when a three-phase fault occurs.

V. Conclusion

In this paper, fuzzy logic and neural networks are combined together to propose ANFIS Controller for a HVDC System. The controller uses feed forward neural network architecture. Simulation results clearly show the successful implementation of the adaptive neuro-fuzzy controller (ANFIS) in MATLAB/SIMULINK program simulation package. Following observations can be made from the results; adaptive neuro-fuzzy controller (ANFIS) efficiently updates the rule base with changing system conditions and uses feed forward neural network architecture which has a better performance than conventional PI controller. This work shows the potential ANFIS controller scheme for a HVDC System. And d it is found that ANFIS provide a more intelligent solution to the control of HVDC systems as compared to the conventional PI controller.

Appendix A

Following are the parameters of the HVDC System chosen for the simulation studies:

CIGRE HVDC Benchmark System Data

Parameters	Rectifier	Inverter
AC voltage base	345kV	230kV
Base MVA	100MVA	100MVA
Transf. tap (HV side)	1.01pu	0.989pu
Voltage source	$1.088\angle 22.18^{o}$	$0.935\angle -23.14^{o}$
Nominal DC voltage	500kV	500kV
Nominal DC current	2kA	2kA

References

[1] J. Arrillaga, Y.H. Liu and N.R. Watson, Flexible power transmission—the HVDC options, John Wiley & Sons Ltd, ISBN 978-0-470-05688-2, 2007.

[2] V. K. Sood, HVDC and FACTS Controllers, Kluwer Academic Publishers, ISBN 1-4020-7890-0, 2004.

[3] M. Multani, J. Ren and V.K. Sood, "Fuzzy logic (FL) controlled HVDC system-influence of shape, width & distribution of membership functions (MFs)," Proc. Electrical and Computer Engineering, IEEE CCECE' 10,pp. 1-7, 2-5 May, 2010.

[4] A. Routray, P. K. Dash, and S. K. Panda, "A fuzzy self-tuning PI controller for HVDC links," *IEEE Trans. Power Electron.*, vol. 11, no. 5, pp. 669–679, Sep. 1996.

[5] A. Daneshpooy, A. M. Gole, D. G. Chapman, and J. B. Davies, "Fuzzy logic control for HVDC transmission," *IEEE Trans. Power Del.*, vol.12, no. 4, pp. 1690–1697, Oct. 1997.

[6] P. K. Dash, A. C. Liew, and A. Routray, "High-performance controllers for HVDC transmission links," *Proc. Inst. Elect. Eng., Gen., Transm., Distrib.*, vol. 141, no. 5, pp. 422–428, Sep. 1994.

[7] H. J. C. Peiris, U. D. Annakkage, and N. C. Pahalawaththa, "Damping improvement of an AC-DC interconnected system using fuzzy logic coordinated modulation controller", Energy Management and Power Delivery, vol. 2, pp. 375-380, 1998.

[8] J. Choi, G. Hwang, H.T. Kang and J.H. Park, "Design of fuzzy logic controller for HVAC using an adaptive evolutionary algorithm," Proc. Industrial Electronics, vol. 3, pp. 1816-1821, 2001.

[9] Jyh-Shing and Roger Jang, "ANFIS: Adaptive-network-based fuzzy inference system," *IEEE Trans.Syst., Man, Cybern., vol. 23, no. 3, pp. 665-684, 1993.*

[10] Daneshpooy. A., Gole. A.M., Chapman. D.G. and Davies. J.B., "Fuzzy logic control for HVDC transmission," *IEEE Trans. Power Del.*, vol.12, no.4, pp.1690-1697, Oct 1997.

[11] J. Y. Yoon, "A genetic algorithm approach to design an optimal fuzzy controller for rectifier current control in HVDC system," International Conference on IEEE International Conference on Evolutionary Computation Proceedings, pp.404-409, 1998.

Biographies

M. Ramesh is working as a Associate Professor and HOD, EEE Dept, Medak College of Engineering and Technology, Kondapak Medak Dist, and pursuing Ph.D. at JNT University, Anantapur. He is B.Tech in Electrical & Electronics Engineering and M.Tech in Advanced Power Systems, JNTU, Kakinada. He has many research publications in various international and national journals and conferences. His current research interests are in the areas of HVDC and Power System

A. Jaya Laxmi was born in Mahaboob Nagar District, Andhra Pradesh, on 07-11-1969. She completed her B.Tech. (EEE) from Osmania University College of Engineering, Hyderabad in 1991, M. Tech.(Power Systems) from REC Warangal, Telangana in 1996 and completed Ph.D.(Power Quality) from Jawaharlal Nehru Technological University College of Engineering, Hyderabad in 2007. She has five years of Industrial experience and 13 years of teaching experience. She has worked as Visiting Faculty at Osmania University College of Engineering, Hyderabad and is presently working as Professor, JNTUH College of Engineering, JNTUH, Kukatpally, Hyderabad. She has 40 International Journals to her credit. She has 100 International and National papers published in various conferences held at India and also abroad. Her research interests are Neural Networks, Power Systems & Power Quality. She was awarded "Best Technical Paper Award" for Electrical Engineering in Institution of Electrical Engineers in the year 2006. Dr. A. Jaya laxmi is a Member of IEEE and IAO, Life Member of System society of India, Fellow of Institution of Electrical Engineers Calcutta (M.I.E) and also Life Member of Indian Society of Technical Education (M.I.S.T.E), MIETE, Indian Science Congress.

DSP Algorithm based Enhanced Phase Locked Loop Scheme for DSTATCOM

J. Bangarraju [1] V. Rajagopal [2] A. Jaya Laxmi [3]

Abstract–This paper deals with Enhanced Phase Locked Loop Control scheme for Distributed Static Compensator (DSTATCOM) in the distribution system. The proposed control scheme based DSTATCOM eliminates current harmonics, maintains unity power factor at source, zero voltage regulation and load balancing. The Enhanced Phase Locked Loop (EPLL) Control scheme is based on Digital Signal Processing (DSP) which is used to extract fundamental component of active and reactive currents for generation of reference source currents. The DSTATCOM consists of six-leg based voltage source converter (VSC) which uses uni-polar switching which doubles the switching frequency and reduces size of the filtering circuit. The zig-zag/three single-phase transformers reduce DC bus voltage and acts as a neutral current compensator. The proposed control scheme for six-leg DSTATCOM is modeled and validated in MATLAB R2012b by using simpower systems toolbox.

Keywords–Distributed static compensator (DSTATCOM), unity power factor, zero voltage regulation, enhanced phase locked loop (EPLL), distribution system, resonant converter, simulation, ac analysis.

I. INTRODUCTION

Three phase four wire systems have been used to supply single-phase linear/non-linear loads, such as office automation machines, fans, computer loads, lighting ballasts etc in the distribution systems. These loads in the distribution system experience severe power quality (PQ) problems, such as high reactive power requirement, poor voltage regulation, current harmonics, excessive neutral current, voltage flicker, sag, swell and load unbalancing [1–3]. To limit PQ problems, IEEE and IEC have proposed many standards such as IEEE Std.141-1993, IEEE Std. 519-1992, IEC 1000-3-2 etc. [4–6]. Custom Power Devices (CPDs) are used as solutions for problems discussed in the literature. DSTATCOM is proposed for mitigation of PQ problems in the current, Dynamic Voltage Restorer (DVR) is used for compensating the PQ problems in the voltage whereas the Unified Power-Quality Conditioner (UPQC) is proposed for compensating both current and voltage problems. The DSTATCOM is a shunt connected CPD used for power factor correction, zero voltage regulation, current harmonic suppression and load balancing. The review of control algorithms and its development are discussed in many papers [7–9]. The performance of DSTATCOM mainly depends upon quick extraction of reference currents using control algorithms [10]. Different Phase Locked Loop (PLL) techniques are described for accurate and reliable control [11]. The various classifications of phased locked loops are Parke PLL, adaptive SRF-PLL, multi-complex coefficient-filter based PLL, EPLL, and Power based PLL for various applications [12-16].

In this paper, DSP Algorithm based Enhanced Phase Locked Loop Control Scheme for DSTATCOM is proposed to eliminate the current harmonics, corrects the Power factor, regulates the terminal voltage and balances the source current even when the load currents are unbalanced. The features of DSP based EPLL scheme is

i. Control scheme is simple and hardware implementation in DSP is easy.
ii. EPLL scheme adopts deviations in amplitude of the voltage, phase angle and frequency of input and gives fast accurate response.
iii. It will extract accurate fundamental components from distribution system or supply [17-20].

Three phase four-wire neutral current consists of triplen harmonic currents and zero-sequence neutral currents passing through neutral conductor and hence overloads it. An isolated zig-zag/three single phase transformer is used to mitigate excessive neutral currents [21–23].

II. DSTATCOM SYSTEM CONFIGURATION

The schematic diagram of six-leg VSC based DSTATCOM with EPLL control algorithm is shown in Fig.1. The proposed DSTATCOM is connected at Point of Common Coupling (PCC) of three phase supply having source impedance and three phase linear/non-linear load. The DSTATCOM consists of twelve IGBTs based voltage source converter (VSC) through three interfacing inductors on the ac side and one capacitor on dc side. A six-leg IGBT VSC based requires uni-polar switching and doubles switching frequency so that higher order harmonics can be eliminated by using filter circuit. The DSTATCOM injects compensating currents (i_{ca}, i_{cb}, i_{cc}) in such a way that elimination harmonics, unity power factor at the source, zero voltage regulation and load balancing. A Ripple filter consists of resistance (R_f) and capacitance (C_f) connected across PCC to compensate high frequency voltage harmonics.

The transformer primary winding is connected in zigzag connection and secondary winding is connected to three single phase transformer so as to reduce DC bus voltage. The isolated zigzag/three single phase transformer is used to compensate neutral current. The zigzag transformer is designed in such a way that magneto motive force (mmf) is balanced in all three phases of the transformer. The design and selection of DSTATCOM and zigzag/three single phase transformers is explained in the following section.

The paper first received 16 June 2014 and in revised form 15 Nov 2014.
Digital Ref: APEJ-2012-06-0440

[1,2] Department of Electrical Engineering, B V Raju Institute of Technology, Narsapur, Medak (Dist),Telangana,India,Pin-502313
E-mail: rajujbr@gmail.com,rajsarang@gmail.com
[3] Department of Electrical Engineering, Jawaharlal Nehru Technical University College of Engineering, Kukatpally, Hyderabad,--500085,Telangana, India, E-mail: ajl1994@yahoo.co.in

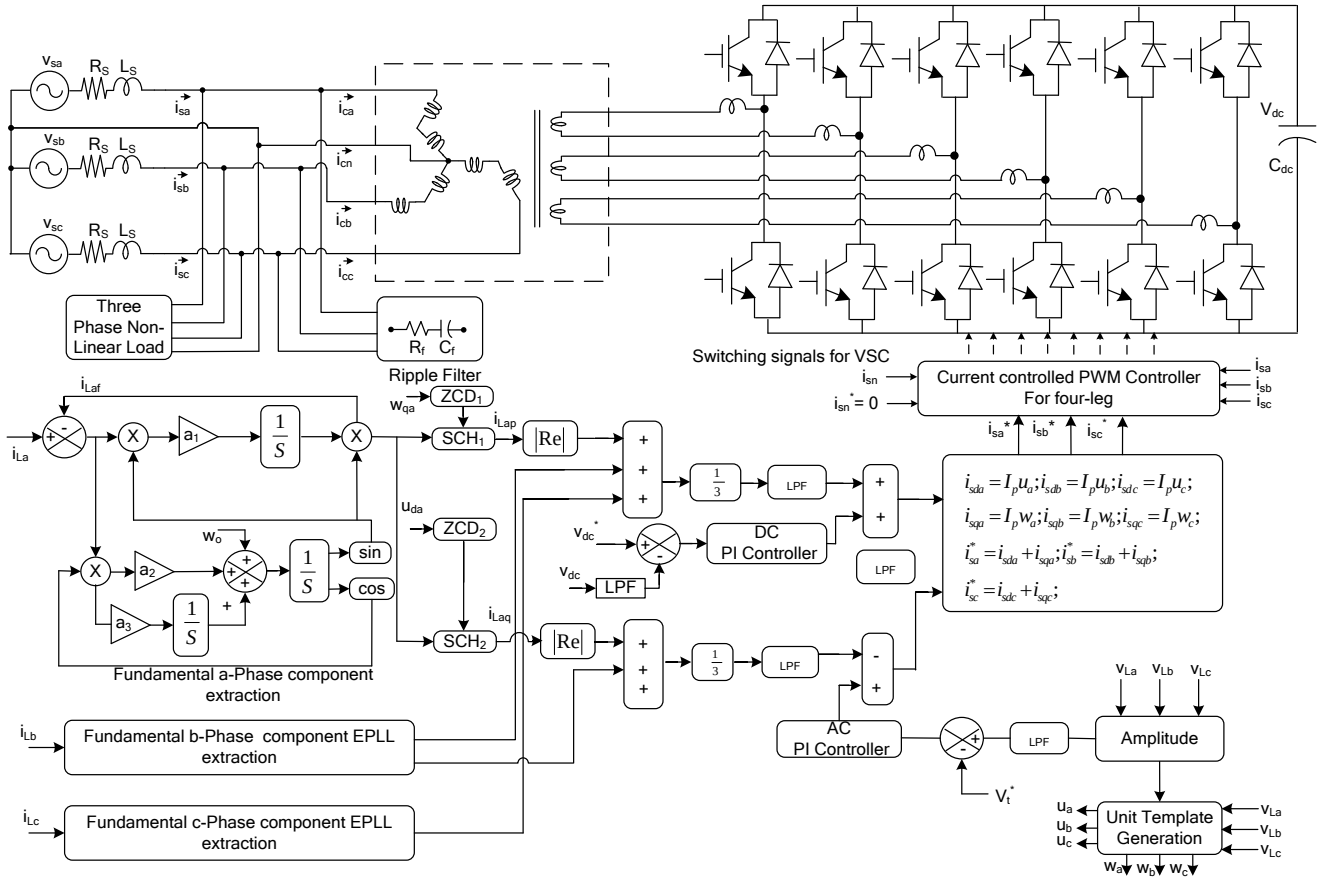

Fig.1 Schematic diagram and control algorithm of six-leg VSC based DSTATCOM

A. Design and selection of zigzag transformer

V_{a1}, V_{a2}, V_{b1}, V_{b2}, V_{c1}, V_{c2} are the voltages across each phase winding and V_a, V_b, V_c are resultant voltages of each phase winding which are shown in Fig. 2.

Assume that input voltage to zig-zag transformer (V_{ab}) =415V then per phase voltage of each winding are $V_{an}=V_{bn}=V_{cn}$=239.6V, $V_{a1}=V_{b1}=V_{c1}$=138.33V and $V_{a2}= V_{b2}= V_{c2}$=138.33V.

B. Design and selection of DSTATCOM

Table.1 shows design and selection values of six-leg DSTATCOM. It consists of DC bus capacitor, DC bus capacitor voltage, ripple filter (R_f and C_f) and Interface inductor(L_{ac}).where V_L is voltage of three phase transformer which is taken as 239.6 V, modulation index (m) is 1, minimum voltage level (V_{mindc}) is 391.26 V, DC bus reference voltage (V_{dc}) is selected as 400V by using zig-zag/three single phase transformer, overloading factor (k) is taken as 1.1, phase current (I_{ph}) is taken as 25 A, phase voltage (V_{ph}) is taken as 239.60 V, time (t) is taken as 250 µs, peak-peak value of current ripple (i_{cp-p}) is taken as 5%, PWM switching frequency (f_s) is taken as 20 kHz , interface ac inductance (L_f) is taken as 2.0 mH, ripple filter series resistance (R_f) is taken as 5 Ω and ripple filter series capacitance (C_f) is taken as 6 µF.

III. PROPOSED CONTROL SCHEME

The dynamic performance of a DSTATCOM is based upon quick and accurate extraction of fundamental component of load currents. Fig.1. shows schematic diagram and Enhanced Phase Locked Loop control Scheme for DSTATCOM to estimate reference source currents. The three-phase supply voltage/phase are v_{sa}, v_{sb}, v_{sc}, three phase supply currents are i_{sa}, i_{sb}, i_{sc}, three phase compensating currents are i_{ca}, i_{cb}, i_{cc}, three phase reference source currents are i_{sa}^*, i_{sb}^*, i_{sc}^*,three phase load currents are i_{La}, i_{Lb}, i_{Lc} and reference DC bus voltage is v_{dc}.

The three phase supply voltages/phase (v_{sa},v_{sb},v_{sc}) can be represented as follows:

$$v_{sa} = v_{mp}\cos(\omega t) \quad (1)$$

$$v_{sb} = v_{mp}\cos(\omega t - 120^\circ) \quad (2)$$

$$v_{sc} = v_{mp}\cos(\omega t - 240^\circ) \quad (3)$$

where v_{mp} is the maximum value of phase supply voltage.

The resultant magnitude of three phase supply voltages can be determined as

$$v_t = \left[2/3\left(v_{sa}^2 + v_{sb}^2 + v_{sc}^2\right)\right]^{1/2} \quad (4)$$

The three supply voltages v_{sa}, v_{sb} and v_{sc} corresponding to in-phase components of unit templates are

$$u_{da} = v_{sa}/v_t, u_{db} = v_{sb}/v_t, u_{dc} = v_{sc}/v_t \quad (5)$$

The three supply voltages v_{sa}, v_{sb} and v_{sc} corresponding to quadrature-phase components of unit templates are

$$w_{qa} = -u_{db}/\sqrt{3} + u_{dc}/\sqrt{3} \quad (6)$$

$$w_{qb} = \sqrt{3}u_{da}/2 + (u_{db} - u_{dc})/2\sqrt{3} \quad (7)$$

$$w_{qc} = -\sqrt{3}u_{da}/2 + (u_{db} - u_{dc})/2\sqrt{3} \quad (8)$$

Table 1: Design and selection of DSTATCOM parameters

Design Parameter	Formulae	Calculated value	Selected value
DC bus Capacitor Voltage	$V_{dc} = 2\sqrt{2}V_L / \sqrt{3}m$	V_{dc}= 391.2652V	V_{dc}=400V
DC Bus Capacitor	$\frac{1}{2}C_{dc}[(V_{dc}^2)-(V_{dc\,\mathrm{mn}}^2)] = 3V_{ph}(kI_{ph})t$	C_{dc} = 2600μF	C_{dc} = 3000μF
Interface AC Inductor	$L_{ac} = (\sqrt{3}mV_{dc})/(12kf_s i_{cp-p})$	L_f=1.9mH	L_f=2.0 mH
Ripple filter	$Z_f = \sqrt{(R_f^2 + X_c^2}$, $X_f = \frac{1}{2\pi f_s L_f}$	Z_f=637Ω	Z_f=637 Ω

The load harmonic currents can be represented by

$$i_{La} = \sum_{k=1}^{\infty} i_{kLa} \cos(k\omega t - \varphi_{ak}) \quad (9)$$

$$i_{Lb} = \sum_{k=1}^{\infty} i_{kLb} \cos(k\omega t - \varphi_{bk} - \frac{2\pi}{3}) \quad (10)$$

$$i_{Lc} = \sum_{k=1}^{\infty} i_{kLc} \cos(k\omega t - \varphi_{ck} + \frac{2\pi}{3}) \quad (11)$$

where i_{kLa}, i_{kLb}, i_{kLc} are the amplitudes of k^{th} harmonic load currents. The Φ_{ak}, Φ_{bk}, Φ_{ck} are the phase angles between supply voltage and k^{th} harmonic load currents.

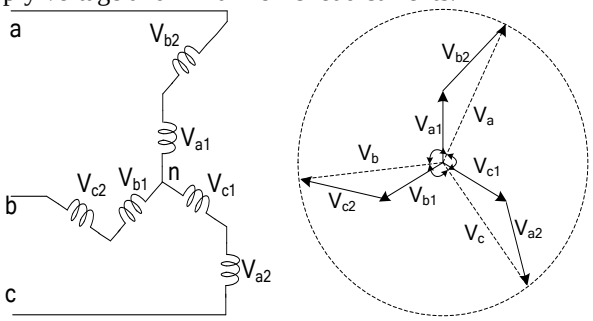

Fig. 2: Zig-zag transformer and phasor diagram

The fundamental load component of each phase current can be estimated by using proposed DSP Algorithm based EPLL control scheme. In this proposed control scheme each phase 'a' extracts input signal from the load current (i_{La}).The error signal (i_{err}) is obtained by the difference between load current (i_{La}) and fundamental load current (i_{Laf}). In this DSP Algorithm based EPLL control scheme internal parameters a_1, a_2 and a_3 are selected as (15), (9) and (1) respectively used to control transient and steady state [17-18]. Similarly other two phase fundamental load currents (i_{Lbf} and i_{Lcf}) are also extracted in the same manner. The phase 'a' fundamental component of load current (i_{Laf}) is in phase with input current signal (i_{La}) and it has phase shift with reference to in-phase unit templates (w_{qa}).

To extract amplitude of reactive power component of fundamental load current, Zero Crossing Detector (ZCD_2) is used on in-phase quadrature templates (u_{da}) are used. The extracted fundamental load current (I_{Laf}) is taken as input to Sample and Hold Circuit (SHC_2) and Zero Crossing Detector (ZCD_2) is used for trigger pulses block. The output of SHC_2 is considered as amplitude of fundamental reactive component load current (I_{Laq}). Similarly other two phase reactive power components of fundamental load current (I_{Lbq} and I_{Lcq}) are also estimated. The average active and reactive power component of fundamental load current is calculated as

$$I_{Lp} = (I_{Lap} + I_{Lbp} + I_{Lcp})/3 \quad (12)$$

$$I_{Lq} = (I_{Laq} + I_{Lbq} + I_{Lcq})/3 \quad (13)$$

These DC component currents are passed through Low Pass Filter (LPF) to extract the active and reactive currents I_{Lp} and I_{Lq}.

i. Unity power factor (UPF) operation of DSTATCOM

The difference between reference DC bus capacitor voltage and actual DC bus voltage of DSTATCOM is taken as error in the DC bus. This error is given to Proportional Integral (PI) controller and output of PI is considered as current loss component (I_{lsp}) and is added to active component of current (i_{Lp}).

$$I_{lsp(m)} = I_{lsp(m-1)} + K_{dp}(V_{dc(m)} - V_{dc(m-1)}) + K_{di}V_{dc(m)} \quad (14)$$

where the error in DC bus at m^{th} sample instant is given by $V_{dc(m)}=V_{dc}^{*}-V_{dc(m)}$. The K_{dp} and K_{di} are proportional and integral constants of PI controller.

The reference active component of source current is calculated as

$$I_p = I_{Lp} + I_{lsp} \quad (15)$$

ii. Zero voltage Regulation operation of DSTATCOM

The source current delivers same active component current I_p along with reactive power component I_q. The difference between actual amplitude of terminal voltage at PCC (V_t) and reference terminal voltage is taken as error at the AC bus.

$$I_{lsp(m)} = I_{lsp(m-1)} + K_{qp}(V_{t(m)} - V_{t(m-1)}) + K_{qi}V_{t(m)} \quad (16)$$

where the error in AC bus at m^{th} sample instant is given by $Vt_{(m)}=V_t^{*}-V_{t(m)}$. The K_{qp} and K_{qi} are proportional and integral constants of PI controller. This error is given to Proportional Integral (PI) controller and output of PI is considered as current loss component (I_{lsq}) and added to active component current (I_{Lq}).

$$I_q = I_{Lq} - I_{lsq} \quad (17)$$

iii. Reference source currents estimation and generation of gating pulses

The three phase reference active and reference source currents can be generated by using in-phase unit templates,

quadrature unit templates, active power component and reactive power components.

$$i_{sda} = I_p u_{da}, i_{sdb} = I_p u_{db}, i_{sdc} = I_p u_{dc} \quad (18)$$

$$i_{sqa} = I_q u_{qa}, i_{sqb} = I_q u_{qb}, i_{sqc} = I_q u_{qc} \quad (19)$$

The three phase reference source currents (i_{sa}^*,i_{sb}^*,i_{sc}^*) can be generated by

$$i_{sa}^* = i_{sda} + i_{sqa} \quad (20)$$

$$i_{sb}^* = i_{sdb} + i_{sqb} \quad (21)$$

$$i_{sc}^* = i_{sdc} + i_{sqc} \quad (22)$$

iv. Current Controlled PWM Generator for six-leg VSC

The error currents are obtained by the difference between reference source currents (i_{sa}^* , i_{sb}^* , i_{sc}^*) and source currents (i_{sa} , i_{sb} , i_{sc}). The equations are given by

$$i_{aer} = i_{sa}^* - i_{sa} \quad (23)$$

$$i_{ber} = i_{sb}^* - i_{sb} \quad (24)$$

$$i_{cer} = i_{sc}^* - i_{sc} \quad (25)$$

To generate uni-polar gating pulses for six-leg VSC, the error-current signals (i_{aer},i_{ber}, i_{cer}) are compared with triangular wave (i_{tri}). The uni-polar switching doubles the PWM switching frequency so that it reduces the filter circuit requirement and improves performance of DSTATCOM.

$i_{aer} > i_{tri}$ (phase 'a' in the left-leg VSC upper switch is on)
$i_{aer} \leq i_{tri}$ (phase 'a' in the left-leg VSC lower switch is on)
$-i_{aer} > i_{tri}$ (phase 'a' in the right-leg VSC upper switch is on)
$-i_{aer} \leq i_{tri}$ (phase 'a' in the right-leg VSC lower switch is on)
Similar logic is used for other two phases of H-bridge VSC.

v. Computation of PI Controller Gains

The DC and AC PI controller gains constants obtained using the Ziegler–Nichols step response technique. A step input of amplitude (U) is applied and the output response of the dc bus voltage is obtained for the open-loop system. The maximum gradient (G) and the point at which the line of maximum gradient crosses the time axis (T) are computed. The gains of the controller are computed using the following equations:

$$K_p = \left|1.2U / GT\right| \quad (26)$$

$$K_p = \left|0.6U / GT^2\right| \quad (27)$$

The gain values for both the DC and AC PI controllers are computed and are given in the Appendix.

IV. Simulation Results and Discussion

DSP Algorithm based EPLL control scheme based DSTATCOM along with zig-zag/three single phase transformer is modeled using MATLAB and simulation results are demonstrated for unity power factor, zero voltage regulation, elimination of harmonics, neutral current compensation and load balancing for three linear/non-linear loads.

A. Performance of EPLL control scheme based DSTATCOM with linear loads for neutral current compensation and UPF operation

The dynamic performance of EPLL control scheme based DSTATCOM with linear loads balanced/unbalanced condition under UPF operation is depicted in Fig. 3. At t=0.75 sec, three phase load is changed to two phase load and at t= 0.85 sec again two phase load is changed to three phase load. The three phase supply voltages (v_{sa} ,v_{sb} ,v_{sc}), source currents (i_{sa},i_{sb},i_{sc}), load currents (i_{La},i_{Lb},i_{Lc}), compensating currents (i_{ca},i_{cb},i_{cc}), source neutral current (i_{sn}), load neutral current (i_{Ln}), DC bus voltage (v_{dc}) and terminal voltage(v_t) are depicted in Fig.3. At different variations in three phase load, it is observed that supply voltages, source currents are balanced and harmonic free, supply neutral current is almost zero, DC bus voltage is maintained close to reference DC bus voltage of 400V and unity power factor at the source voltage and source current .

B. Performance of EPLL control scheme based DSTATCOM with non-linear loads for neutral current compensation and UPF operation

The dynamic performance of EPLL control scheme based DSTATCOM with Non-linear loads balanced/unbalanced condition under UPF operation is depicted in Fig. 4. At t=0.75 sec, three phase load is changed to two phase load and at t= 0.85 sec again two phase load is changed to three phase load. The three phase supply voltages (v_{sa}, v_{sb}, v_{sc}), source currents (i_{sa}, i_{sb}, i_{sc}), load currents (i_{La}, i_{Lb}, i_{Lc}), compensating current (i_{ca},i_{cb},i_{cc}),source neutral current (i_{sn}), load neutral current(i_{Ln}),DC bus voltage(v_{dc}) and terminal voltage(v_t) are depicted in Fig .4. At different variations in three phase load it was observed that supply voltages, source currents are balanced and harmonic free, supply neutral current is almost zero, DC bus voltage is maintained close to reference DC bus voltage of 400V and unity power factor at the source voltage and source current. The source voltage and source current THDs are 2.59% and 2.78% whereas load THD is 91.55%.

C. Performance of EPLL control scheme based DSTATCOM with linear loads for neutral current compensation and zero voltage regulation operation

The dynamic performance of EPLL control scheme based DSTATCOM with linear loads balanced/unbalanced condition under zero voltage regulation operation is depicted in Fig. 5. At t=0.75 sec, three phase load is changed to two phase load and at t= 0.85 sec again two phase load is changed to three phase load. The three phase supply voltages (v_{sa},v_{sb},v_{sc}), source currents(i_{sa},i_{sb},i_{sc}), load currents (i_{La},i_{Lb},i_{Lc}), compensating current (i_{ca},i_{cb},i_{cc}) source neutral current (i_{sn}), load neutral current (i_{Ln}), DC bus voltage (v_{dc}) and terminal voltage (v_t) are depicted in Fig .5. At different variations in three phase load it is observed that supply voltages, source currents are balanced and harmonic free, supply neutral current is almost zero, unity power factor at the source, DC bus voltage and voltage at PCC are maintained close to reference values of 400V and 339 V respectively.

D. Performance of EPLL control scheme based DSTATCOM with Non-linear loads for neutral current compensation and zero voltage regulation operation

The dynamic performance of EPLL control scheme based

DSTATCOM with non-linear loads balanced/unbalanced condition under zero voltage regulation operation is depicted in Fig. 6. At t=0.75 sec, three phase load is changed to two phase load and at t= 0.85sec again two phase load load is changed to three phase load. The three phase supply voltages (v_{sa}, v_{sb}, v_{sc}), source currents (i_{sa}, i_{sb}).

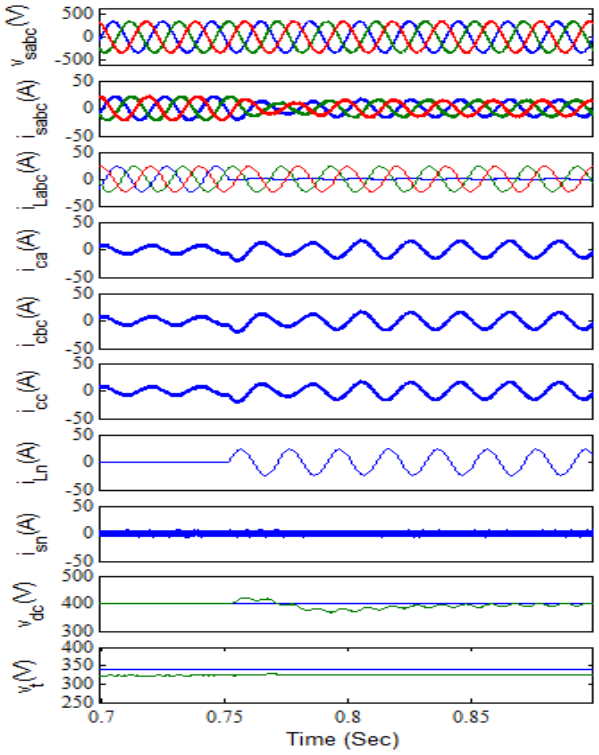

Fig. 3: Performance of DSP algorithm based EPLL control scheme for DSTATCOM with linear loads under UPF operation.

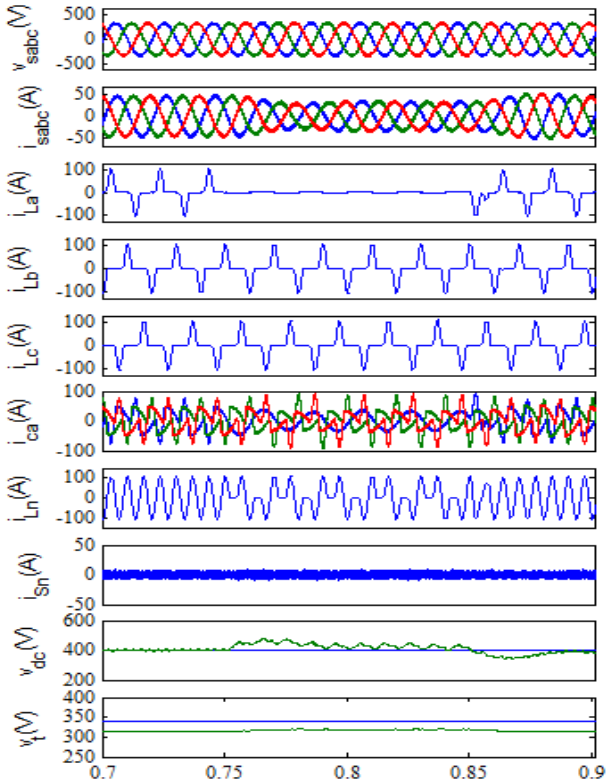

Fig. 4: Performance of DSP algorithm based EPLL control scheme for DSTATCOM with non-linear loads under UPF operation.

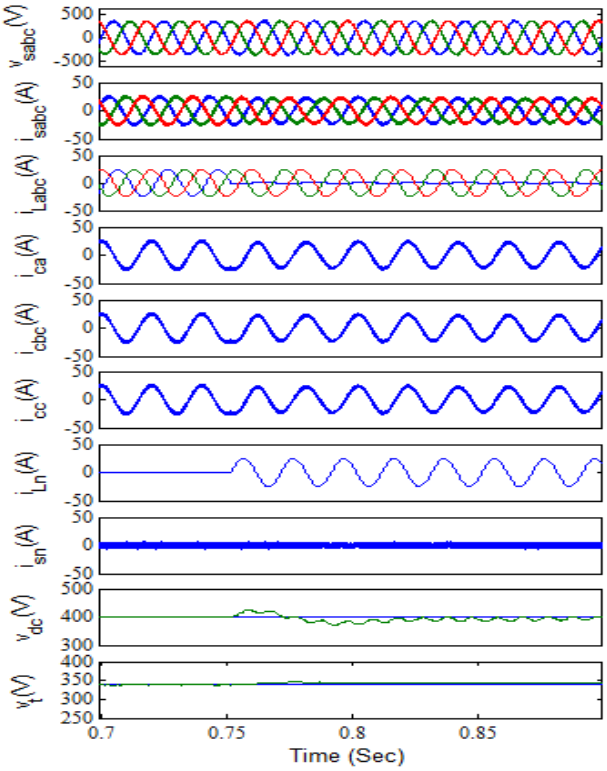

Fig. 5: Performance of DSP algorithm based EPLL Control scheme for DSTATCOM with linear loads under zero voltage regulation operation.

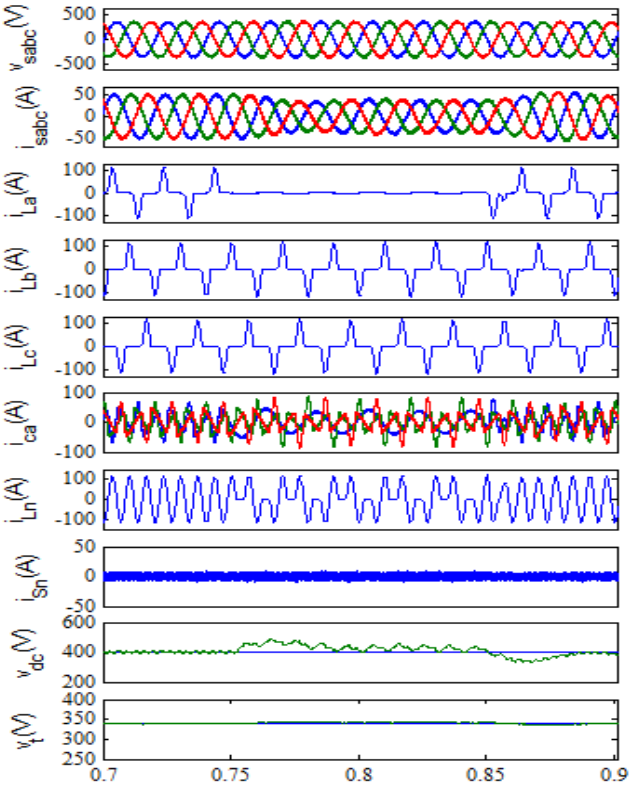

Fig. 6: Performance of DSP Algorithm based EPLL Control scheme for DSTATCOM with non-linear loads under zero voltage regulation operation

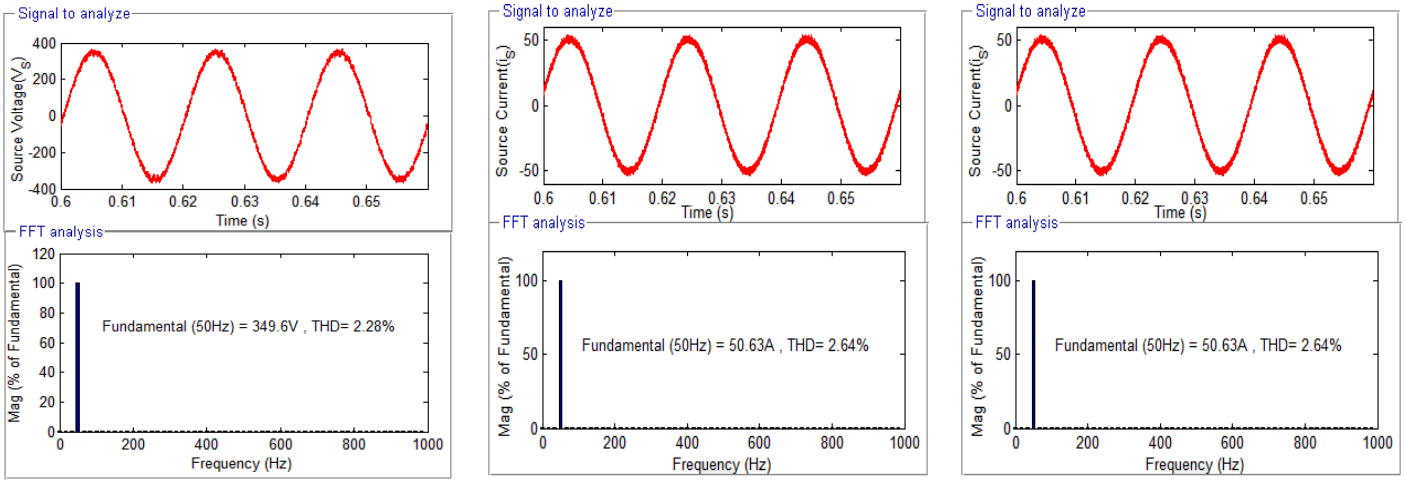

Fig. 7: Harmonic spectra of source voltage, source current and load current.

i_{sc}),load currents (i_{La}, i_{Lb}, i_{Lc}), compensating current(i_{ca}, i_{cb}, i_{cc}), source neutral current (i_{sn}), load neutral current (i_{Ln}), DC bus voltage (v_{dc}) and terminal voltage (v_t) are depicted in Fig .6. At different variations in three phase load it was observed that supply voltages, source currents are balanced and harmonic free, supply neutral current is almost zero, unity power factor at the source, DC bus voltage and voltage at PCC are maintained close to reference values of 400V and 339V respectively. The source voltage and source current THD are 2.28% and 2.64% whereas load THD is 91.85% are shown in Fig.7.

VI. Conclusion

The dynamic performance of DSP Algorithm based EPLL control scheme for six-leg VSC based DSTATCOM with linear/non-linear loads gives satisfactory results. The performance of DSTATCOM demonstrated for neutral current compensation under unity power factor and zero voltage regulation modes along with harmonic elimination. The zigzag/three single phase transformers has maintained source neutral current which is almost equal to zero and act as a neutral current compensator. The six-leg VSC uses uni-polar switching which doubles frequency so that filter requirement is reduced. The DC bus voltage is regulated to reference value of 400V in all variations of loads during unity power factor and zero voltage regulation operation. The terminal voltage is regulated to reference value of 339V in all variations of load during zero voltage regulation. The three phase non-linear load draws a load current of total harmonic distortion (THD) of 91.85% whereas source voltage and current are having a THD of 2.28% and 2.64% respectively. These THDs of source voltage and source currents are within the limits of IEEE-519 & IEC 1000-3-2 standards.

Appendix

Three phase supply line voltage: 415V, 50Hz
Supply Impedance: R_s=0.04Ω, L_s=4mH
Loads:
i. *Linear load*: R_L=12 Ω and L=25mH
ii.*Non-linear loads*: *Three single phase diode bridge rectifier with R*=12 Ω and *C*=500 µF
Ripple filter at PCC: R_f=5 Ω and C_f=5µF
DSTATCOM:
DC bus capacitor C_{dc} =3000 µF
DC bus Voltage: 400V
DC bus voltage PI controller: K_{dp}=0.5, K_{di}=0.8
AC bus voltage PI controller: K_{qp}=1.02, K_{qi}=0.65
PWM switching frequency: 20 kHz.

References

[1] A. Ghosh and G. Ledwich, "Power Quality Enhancement using Custom Power devices", Kluwer Academic Publishers, London, 2002.
[2] R. C. Dugan, M. F. McGranaghan and H. W. Beaty, "Electric Power Systems Quality", 2nd Edition, New York, McGraw Hill, 2006.
[3] M. H. J. Bollen, "Understanding Power Quality Problems: Voltage Sags and Interruptions", ser. IEEE Press Power Eng. Piscataway, NJ: IEEE, 2000.
[4] "IEEE Recommended Practice for Electric Power Distribution for Industrial Plants", IEEE Std. 141, 1993.
[5] "IEEE Recommended Practices and Requirements for Harmonics Control in Electrical Power Systems", IEEE Std.519, 1992.
[6] "Electromagnetic Compatibility (EMC)—Part 3: Limits-Section 2: Limits for Harmonic Current Emissions (Equipment Input Current>16A per Phase)", IEC1000-3-2 Document1st ed., 1995.
[7] F. Barrero, S. Mart ńez, F. Yeves, and P. M. Martinez, "Active power filters for line conditioning: A critical evaluation", *IEEE Trans. on Power Del.*, vol. 15, no. 1, pp. 319-325, Jan. 2000.
[8] A. M. Massoud, S. J. Finney, and B. W. Williams, "Review of harmonic current extraction techniques for an active power filter", in Proc. 11th Int. Conf. Harmonies Quality Power, pp. 154-159, 2004.
[9] L. Sainz and J. Balcells, "Harmonic interaction influence due to current source shunt filters in networks supplying nonlinear loads", *IEEE Trans. on Power Del.*, vol. 27, no. 3, pp. 1385-1393, Jul. 2012.
[10] B. Singh and J. Solanki, "A comparison of control algorithms for DSTATCOM", *IEEE Trans .on Ind. Electron.*, vol. 56, no. 7, pp. 2738-2745, Jul. 2009.
[11] G. Chyun, G. C. Hsieh and J. C. Hung, "Phase-locked loop techniques-A survey", *IEEE Trans. on Ind. Electron.*, vol. 43, no. 6, pp.609-615, Dec. 1996.
[12] F. Gonzalez-Espín, E. Figueres, and G. Garcera, "Garcera, An adaptive Synchronous reference frame phase-locked loop for power quality improvement in a polluted utility grid", *IEEE Trans. on Ind. Electron*., vol.59, no.6, pp.2718-2731, Jun.2012.

[13] C. H. da Silva, R. R. Pereira, L. E. B. da Silva, G. Lambert-Torres, B. K. Bose and S. U Ahn, "A digital PLL scheme for three-phase system using modified synchronous reference frame", *IEEE Trans. on Ind. Electron.*, vol.57, no.11, pp.3814-3821, Nov.2010.

[14] X. Guo, W. Wu and Z. Chen, "Multiple-complex coefficient-filter based phase-locked loop and synchronization technique for three-phase grid-interfaced converters in distributed utility networks", *IEEE Trans. Ind. on Electron.*,vol.58, no.4, pp.1194-1204, Apr.2011.

[15] P. Karuppanan and K. K. Mahapatra, "PLL with fuzzy logic controller based shunt active power filter for harmonic and reactive power compensation", in Proc. India Int. Conf. Power Electron., pp. 1-6, 2011.

[16] F. Liccardo, P. Marino and G. Raimondo, "Robust and fast three-phase PLL tracking system", *IEEE Trans. Ind. on Electron.*, vol. 58, no. 1, pp. 221-231, Jan.2011.

[17] M. K. Ghartemani, B. T. Ooi, and A. Bakhshai, "Application of enhanced phase-locked loop system to the computation of synchrophasors," *IEEE Trans. on Power Del.*, Vol. 26, No. 1, pp. 22-32, Jan. 2011.

[18] M. K. Ghartemani, H. Mokhtari, M. R. Iravani, and M. Sedighy, "A signal processing system for extraction of harmonics and reactive current of single-phase systems", *IEEE Trans. on Power Del.*, vol. 19, no. 3, pp. 979-986, Jul.2004.

[19] M. Karimi-Ghartemani and M. R. Iravani, "A method for synchronization of power electronic converters in polluted and variable-frequency environments", *IEEE Trans. on Power Syst.*, vol.19, no.3, pp.1263-1270, Aug. 2004.

[20] B.Singh and Sabha Raj Arya, "Implementation of Single-Phase EnhancedPhase-Locked Loop-Based Control Algorithm for Three-Phase DSTATCOM", *IEEE Trans. on Power Del.*, vol. 28, no. 3, pp. 1516-1524, Jul.2013.

[21] Bhimsingh, P.Jayaprakash, T.R.Somayajulu and D.P.Kothari, "Reduced Rating VSC With a Zig-Zag Transformer for Current Compensation in a Three-Phase Four-Wire Distribution System", *IEEE Trans. on Power Electron.*, vol. 24, no. 1, pp.249-259, Jan. 2009.

[22] B. A. Cogbill and J. A. Hetrick, "Analysis of T–T connections of two single phase transformers," *IEEE Trans. on Power App. Syst.*, vol. PAS-87, no.2, pp.388-394, Feb.1968.

[23] Bhimsingh, P. Jayaprakash and D. P. Kothari, "A T-Connected Transformer and Three leg VSC based DSTATCOM for Power Qualitys Improvement", *IEEE Trans. on Power Electron.*, vol. 23, no. 6, pp.2710-2718, Nov. 2008.

BIOGRAPHIES

J. Bangarraju was born in Tanuku, India, in 1982.He received the B. Tech. degree in Electrical and Electronics Engineering from A.S.R College of Engineering, Tanuku in 2004 and the M.Tech degree from JNTU, Hyderabad in 2007. Presently working as Associate Professor in B V Raju Institute of Technology, Narsapur, Telangana, India. His area of interest includes Power Electronics and Drives, Power Quality, FACTS and Artificial neural networks. He is currently working towards Ph.D degree at the Department of Electrical Engineering, JNTU Hyderabad, India. He is a life member of the Indian Society for Technical Education (ISTE) and Member of the Institute of Electrical and Electronics Engineers (IEEE).

V. Rajagopal was born in Kazipet, Warangal, India, in 1969. He received the AMIE (Electrical) degree from The Institution of Engineers (India), in 1999, M.Tech. Degree from the Uttar Pradesh Technical University India, in 2004 and Ph D degree in Indian Institute of Technology (IIT) Delhi India , in 2012.Presently working as Professor in B V Raju Institute of Technology, Narsapur, Telangana, India. His area of interest includes power electronics and drives, renewable energy generation and applications, FACTS, and power quality. He is a life member of the Indian Society for Technical Education (ISTE) and the Institution of Engineers (India) (IE (I)) and a Member of the Institute of Electrical and Electronics Engineers (IEEE).

A. Jaya Laxmi was born in Mahaboob Nagar District, Andhra Pradesh, on 07-11-1969. She completed her B.Tech. (EEE) from Osmania University College of Engineering, Hyderabad in 1991, M. Tech.(Power Systems) from REC Warangal, Andhra Pradesh in 1996 and completed Ph.D.(Power Quality) from Jawaharlal Nehru Technological University, Hyderabad in 2007. She has five years of Industrial experience and 14 years of teaching experience. Presently, working as Professor, Electrical & Electronics Engg., and Coordinator, Centre for Energy Studies, JNTUH College of Engineering, Jawaharlal Nehru Technological University Hyderabad, Kukatpally, and Hyderabad. She has 45 International Journals to her credit and also has 100 International and National papers published in various conferences held at India and also abroad. Her research interests are Neural Networks, Power Systems & Power Quality. She was awarded "Best Technical Paper Award" in Electrical Engineering from Institution of Electrical Engineers in the year 2006. Dr. A. Jaya laxmi is a Member of IEEE, Member of International Accreditation Organization (M.I.A.O), Fellow of Institution of Electrical Engineers Calcutta (F.I.E), Life Member of System Society of India (M.S.S.I), Life Member of Indian Society of Technical Education (M.I.S.T.E), Life Member of Electronics & Telecommunication Engineering (M.I.E.T.E), Life Member of Indian Science Congress (M.I.S.C).

Boundary Control of a Buck Converter with Second-Order Switching Surface and Conventional PID Control- A Comparative Study

P. Kumar [1]

Abstract–This paper presents a comparative study of boundary control of a buck converter with second-order switching surface and conventional PID control. Fixed frequency boundary control technique is based on the concept of integrating variable hysteresis and second-order switching surface incorporated into boundary control technique.PID control is a very popular conventional technique which gives linear control for the buck converter. Both the control methods have been implemented for a 140W, 24V/12V buck converter. The basic operating principles and stability analysis, design parameters will be given for both the controllers. The steady state characteristics, output voltage ripple and efficiency of the converter will be discussed under very large disturbances like change in input voltages and output loads. Simulink model of each individual parts like second-order boundary control, Frequency to voltage converter, hysteresis band has been given. The system responses under large signal supply voltage and load disturbances have been verified by MATLAB/SIMULINK.

Keywords–PID control, second-order boundary control, buck converter, Matlab/simulink.

I. INTRODUCTION

Controlling a switched power converter resembles a wide area of research in control technology. Most of the electronic devices operate at some input supply usually constant in nature. With the increase in circuit complexity and improved technology a more severe requirement for accurate and fast regulation is desired. This has led to need for a newer and more reliable design of controllers which can have faster response with better performance. In general a dc-dc converter inputs are unregulated dc voltage input and outputs a constant or regulated voltage.

A boundary control technique builds on a state-space representation of a converter's operation. In state space, the vector of inductor currents and capacitor voltages evolves over time and subsequent points form a system trajectory. When switch action is made dependant on the state, the control law can be represented as a switching surface [1]. Boundary control is a large-signal tool for the design and analysis of switching power converters. A boundary control splits the state space of a given converter with a switching surface, such that on one side of the boundary, the converter operation is governed by on-state trajectories and on the other side off-state trajectories are followed [2], [3]. Boundary control techniques with linear switching surfaces, such as hysteresis control and sliding-mode control [1], [2], [4], or nonlinear switching surfaces to pulse width-modulated control strategies in dc/dc switching regulators. It addresses the complete operation of a converter and does not differentiate startup, transient, and steady-state periods[1], [10].

Several commonly used methods for reducing of switching frequency of static power converters are coupled to a sliding mode controller. Sliding mode control methods have been used earlier to operate power converter at its finite switching frequency, but it also results some error as control system operates at finite switching frequency[11], [12]. Similarly, pulse modulation based sliding mode control can also be used to operate converter at its fixed frequency[13]. Two novel approaches adopting the sliding mode concept can be used to make the system tracking reference inputs. Phase currents and the neutral point voltage are controlled simultaneously[14].

As we know, the error increases as the converter's switching frequency decreases as the same integral sliding mode control becomes ineffective in reducing the steady state error which has been earlier used to suppress the steady state error through incorporating additional integral term of state variable into the controller [15]. The ripple control is the simplest among all switching regulators. Main advantages of the ripple regulator, like other variable frequency regulators, are fast transient response, unconditional stability, and wide range of output/input voltages. But the switching frequency depends on the operating conditions and power filter [16].

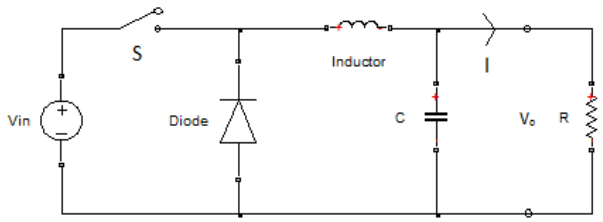

Fig. 1: Buck converter topology

II. BUCK CONVERTER MODELING

In Fig.1 a dc-dc buck converter is shown. The buck converter circuit converts a higher dc input voltage to lower dc output voltage. It consists of a controlled switch *S*, an uncontrolled switch *D* (diode), an inductor *L*, a capacitor *C*, and a load resistance R. In the description of converter operation, it is assumed that all the components are ideal and also the converter operates in CCM. In CCM operation, the inductor current flows continuously over one switching period. When the switch *S* is ON and diode *D* is reverse biased, the dynamics of inductor current I_L and the capacitor voltage V_C are

The paper first received 20 June 2014 and in revised form 17 Nov 2014.
Digital Ref: APEJ-2014-6-442
[1] Department of Electrical Engineering, Indian Institute of Technology (BHU)
E-mail: piyushkumar.nitw@gmail.com

$$\frac{dI_L}{dt}=\frac{1}{L}\left(V_{in}-V_o\right) \text{ and } \frac{dV_o}{dt}=\frac{dV_c}{dt}=\frac{1}{C}I_c \quad (1)$$

when the switch S is off and D is forward biased, the dynamics of the circuit are

$$\frac{dI_L}{dt}=-\frac{1}{L}V_o \text{ and } \frac{dV_o}{dt}=\frac{dV_c}{dt}=\frac{1}{C}I_c \quad (2)$$

Table 1: Buck converter design parameters

Parameters	Values
L	100 µH
R	1.2/2.4 ohm
C	400 µF
Vin	20-30V

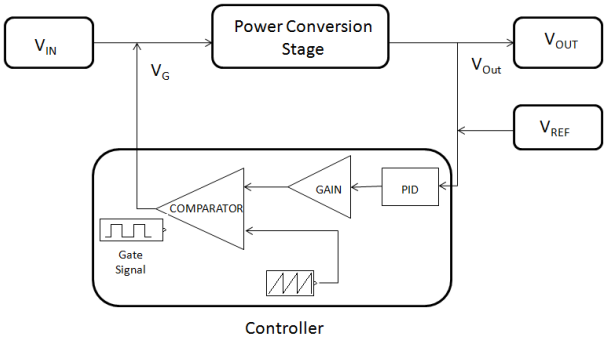

Fig. 2: System block diagram for PID controller

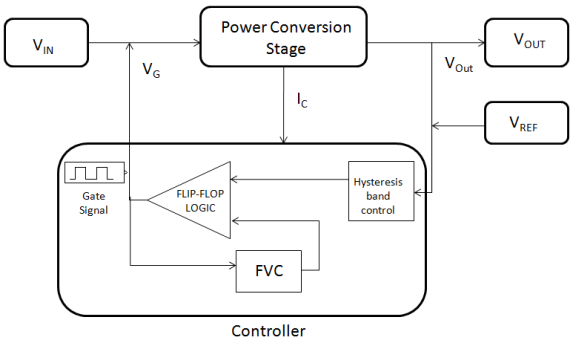

Fig. 3: System block diagram for SBC controller

III. Control Techniques

Fig. 2 and Fig. 3 shows the part-wise system block diagram for the implementation of PID and SBC controllers during buck converter application respectively.

A. Second-order boundary control implementation

It consists of four major parts, including the main power conversion stage (PCS), the second-order boundary controller (SBC) [5]–[7], the frequency-to-voltage converter (FVC), and the error amplifier (EA).

FVC firstly converts the gate signal V_G for PCS into a dc voltage V_{FVC}, which will then be compared with a reference voltage $V_{f,ref}$ by EA. The output of EA, Δ, is used to control the hysteresis band. SBC inside will generate upper and lower bands together with Δ to determine the switching times of the main switch S in PCS. Thus, the function of SBC is used to regulate the output voltage and the earlier mentioned four parts form a feedback loop for regulating the switching frequency [9].

B. Frequency to voltage converter

In Fig. 4 simulink model of FVC is shown. FVC presence helps in operating the system at its fixed frequency. It generates the necessary voltage which is proportional to the frequency. It governs the system to operate close to its fixed frequency by detecting the change in δV_f which will be in proportion to δf_s.

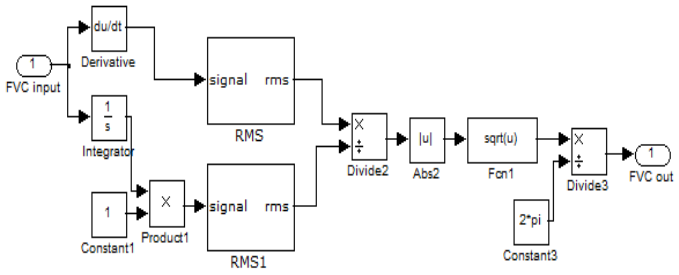

Fig. 4: Frequency to voltage converter model

C. PID controller

The PID controller involves three separate constant parameters the proportional, the integral and derivative values, denoted by P, I, and D. Control signal of PID controller is denoted by

$$u(t)=ke(t)+\int_0^t k_i(\tau)d\tau+k_d\frac{\partial e(t)}{\partial t} \quad (3)$$

Control parameters assumed for PID control implementation are K_p=1.26, K_i=0.003 and K_d=2.23 respectively.

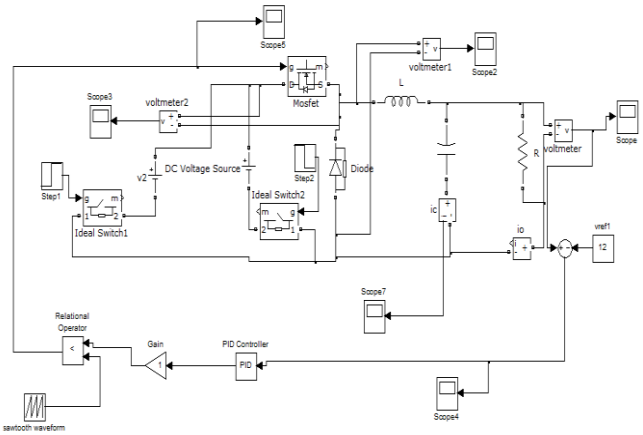

Fig. 5: Matlab/Simulink implementation of a PID controller

IV. Simulation Result Verification

140 W buck converter has been tested with both control techniques and the specifications are given as follows:

a. input voltage,V_{in} : 20–30V
b. output voltage,V_0: 12V
c. maximum output voltage ripple, 2 V
d. maximum inductor current ripple: 7 A

Fig. 5 and Fig. 6 show the simulink model implementation of PID controller and SBC controller respectively. Fig. 7 to Fig. 10 show the waveforms of the output voltage and the load current when the input voltage is changed suddenly from 20V to 30V and vice versa, respectively. As observed in the waveform, the maximum and minimum output voltage ripple obtained with PID are 12.68V and 11.04V respectively while with SBC the maximum and

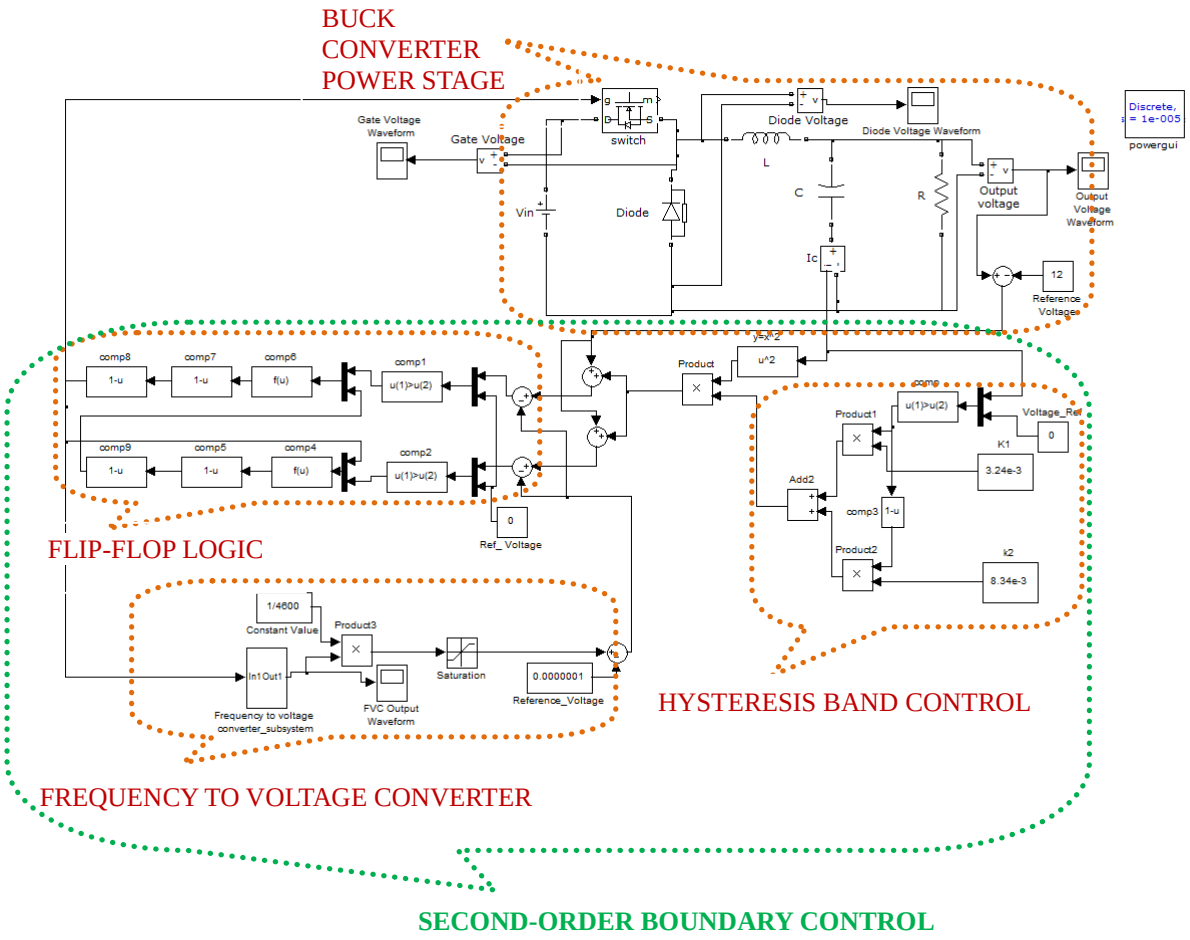

Fig. 6: Matlab/Simulink implementation of second-order boundary (SBC) control of a Buck converter

minimum output voltage ripple obtained are 12.02V and 11.96V respectively. Therefore, there is overall 96.3% improvement in the output voltage ripple after the occurrence of disturbance with SBC control algorithm. Similarly, there is a 95.6% improvement in load current ripple with the use of SBC.

Fig. 11 to Fig. 14 show the waveforms when the load resistance change from 1.2 Ω (10A, 120W) to 2.4 Ω (5A, 60W), and vice versa, respectively.

For better understanding, the maximum and minimum voltage and load current obtained under all possible disturbance considered are duly tabulated in Table-II. With the use of PID controller there is a large fluctuation in output voltage and load current ripple during and after disturbances, whereas SBC controller keeps current and voltage ripple almost constant throughout during and after the disturbance.

For SBC control, the transient periods last about 40 μs and 50 μs,. Again, the converter settles in two switching actions and the steady-state switching period is also kept at about 40 μs before and after the two input disturbances. The input voltage is introduced with a high percentage of ripples.

Apart from studying the dynamic response, it can be observed that the output voltage can be regulated tightly at the steady state without being affected by the input voltage ripple. Whereas PID control takes more time to settle showing more ripple content during all type of transient period.

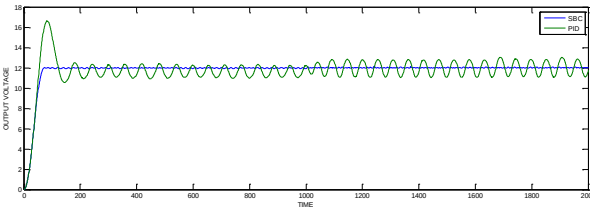

Fig. 7: Sudden change in input V_i from 30V to 20V

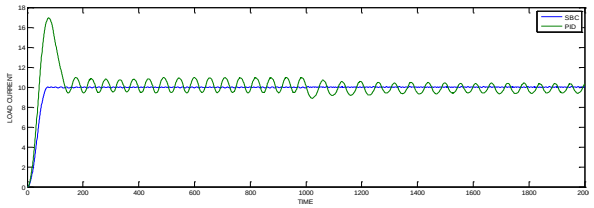

Fig. 8: Sudden change in input V_i from 30V to 20V

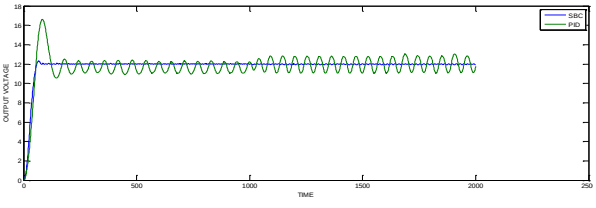

Fig. 9: Sudden change in input V_i from 20V to 30V

Table 1I: Comparative results index in terms of output ripple for SBC and PID control implemented in a buck before and after disturbance

Quantity changed	*Parameters*	*Ripple* Δ	*Output ripple with PID*		*Output ripple with SBC*	
			before	**after**	**before**	**after**
Input voltage (30V to 20V)	Output voltage	Maximum	12.24	12.82	12.04	12.04
		Minimum	11.08	11.1	11.95	11.94
	Load current	Maximum	10.25	10.68	10.07	10.07
		Minimum	9.163	9.226	9.93	9.93
Input voltage (20V to 30V)	Output voltage	Maximum	13.15	12.68	12.02	12.02
		Minimum	11.34	11.04	11.95	11.96
	Load current	Maximum	10.96	10.57	10.04	10.02
		Minimum	9.448	9.19	9.993	9.96
Load 2.4Ω (5A, 60W) to 1.2Ω (10A, 120W)	Output voltage	Maximum	12.33	12.67	12.03	12.02
		Minimum	11.73	11.27	11.94	11.97
	Load current	Maximum	5.16	10.58	5.013	10.02
		Minimum	4.89	9.25	4.98	9.95
Load 1.2Ω (10A, 120W) to 2.4Ω(5A, 60W)	Output voltage	Maximum	12.67	12.36	12.03	12.06
		Minimum	11.17	11.69	11.98	11.97
	Load current	Maximum	10.55	5.13	10.03	5.02
		Minimum	9.28	4.86	9.93	4.97

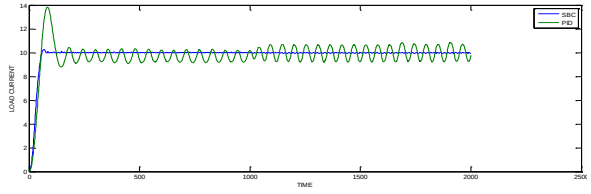

Fig. 10: Sudden change in input V_i from 20V to 30V

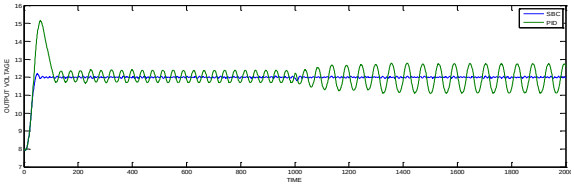

Fig. 11: Sudden load change from 2.4Ω (5A, 60W) to 1.2Ω (10A, 120W)

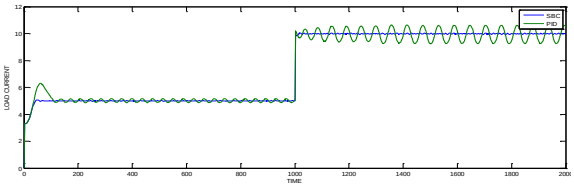

Fig. 12: Sudden load change from 2.4Ω (5A, 60W) to 1.2Ω (10A, 120W)

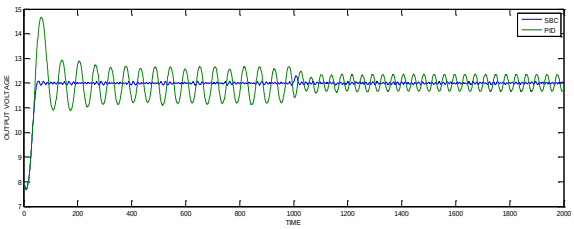

Fig. 13: Sudden load change from 1.2Ω (10A,120W) to 2.4Ω (5A, 60W)

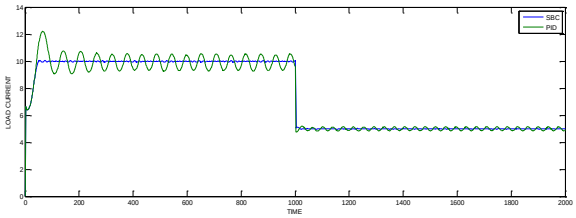

Fig. 14: Sudden load change from 1.2Ω (10A,120W) to 2.4Ω (5A, 60W)

V. Conclusion

Boundary control technique with second-order switching surface and PID control technique for buck converters has been presented and compared. Second-order boundary control exhibits two key features. First, the technique combines the advantage of SBC that the converter can reach the steady state in two switching actions after large-signal disturbances. Second, the switching frequency can be kept at a relatively constant value and the implementation of the frequency control loop only requires simple circuitry. A 140 W prototype has been tested. It can be clearly inferred from the output waveform and comparative table that output ripple variation in PID control seems more as compared to SBC control which has almost similar output ripple before and after the occurrence of external disturbances. In PID control output ripple increases as long as load decreases and this makes the system less efficient as compared to SBC control. Overall there is good agreement between the theoretical predictions and simulation results. As the proposed controller gives a wide range of operation over large disturbances, these can be further extended to other converter topologies.

REFERENCES

[1] R. Munzert, P. T. Krein, M. Carpita, and M. Marchesoni, "Issues in boundary control of power convertors," in PESC Record. 27th Annual IEEE Power Electronics Specialists Conference, vol. 1, no. 5, pp. 810-816, 1996.

[2] M. Greuel, R. Muyshondt, and P. T. Krein, "Design approaches to boundary controllers," in PESC97. Record 28th Annual IEEE Power Electronics Specialists Conference. Formerly Power Conditioning Specialists Conference 1970-71. Power Processing and Electronic Specialists Conference 1972, vol. 1, pp. 672-678, 1997.

[3] W. Yan, C. N. Ho, H. S. Chung, and K. T. K. Au, "Fixed-frequency boundary control of buck converter with second-order switching surface," *IEEE Trans. Power Electron*., vol. 24, no. 9, pp. 2193-2201, Sep. 2009.

[4] W. T. Yan, H. S. H. Chung, K. T. K. Au, and C. N. M. Ho, "Fixed-frequency boundary control of buck converters with second-order switching surface," in 2008 IEEE Power Electronics Specialists Conference, pp. 629-635, 2008.

[5] J. Matas, L. Garcia de Vicuna, J. Miret, J. M. Guerrero, and M. Castilla, "Feedback linearization of a single-phase active power filter via sliding mode control," *IEEE Trans. Power Electron*., vol. 23, no. 1, pp. 116-125, Jan. 2008.

[6] K. K. S. Leung and H. S. H. Chung, "Derivation of a second-order switching surface in the boundary control of buck converters," *IEEE Power Electron. Lett*., vol. 2, no. 2, pp. 63-67, Jun. 2004.

[7] K. S. Leung and H. S. H. Chung, "A comparative study of the boundary control of buck converters using first-and second-order switching surfaces-Part I: continuous conduction mode," in IEEE 36th Conference on Power Electronics Specialists, pp. 2133-2139, 2005.

[8] M. Ordonez, M. T. Iqbal, and J. E. Quaicoe, "Selection of a curved switching surface for buck converters," *IEEE Trans. Power Electron.*, vol. 21, no. 4, pp. 1148-1153, Jul. 2006.

[9] K. K. Leung and H. S. Chung, "A comparative study of boundary control with first- and second-order switching surfaces for buck converters operating in DCM," *IEEE Trans. Power Electron*., vol. 22, no. 4, pp. 1196-1209, Jul. 2007.

[10] S. Banerjee and G. C. Verghese, Nonlinear Phenomena in Power Electronics. IEEE, pp. 472, 2001.

[11] B. J. Cardoso, A. F. Moreira, B. R. Menezes, and P. C. Cortizo, "Analysis of switching frequency reduction methods applied to sliding mode controlled DC-DC converters," in Proc. APEC '92 Seventh Annual Applied Power Electronics Conference and Exposition, pp. 403-410, 1992.

[12] M. Carpita and M. Marchesoni, "Experimental study of a power conditioning system using sliding mode control," *IEEE Trans. Power Electron*., vol. 11, no. 5, pp. 731–742, 1996.

[13] Y. M. Lai and C. K. Tse, "A unified approach to the design of PWM-based sliding-mode voltage controllers for basic DC-DC converters in continuous conduction mode," *IEEE Trans. Circuits Syst. I Regul. Pap*., vol. 53, no. 8, pp. 1816–1827, Aug. 2006.

[14] V. Utkin, "Sliding Mode Pulsewidth Modulation," *IEEE Trans. Power Electron.*, vol. 23, no. 2, pp. 619–626, Mar. 2008.

[15] Y.M. Lai and C. K. Tse, "Indirect sliding mode control of power Converters via double integral sliding surface," *IEEE Trans. Power Electron*., vol. 23, no. 2, pp. 600–611, Mar. 2008.

[16] C-H Tso and J-C Wu, "A ripple control buck regulator with fixed output frequency," *IEEE Power Electron. Lett.*, vol. 99, no. 3, pp. 61–63, Sep. 2003.

ACKNOWLEDGMENT

The author would like to thank Dr. B.K. Murthy (Professor at Department of Electrical Engineering, NIT Warangal) for his esteemed guidance and support during entire duration of the project.

BIOGRAPHY

Piyush Kumar obtained his B.Tech degree in Electrical & Electronics Engineering from SRM University, Chennai in the year 2009 and M.Tech in Power electronics & Drives from National Institute of Technology, Warangal in the year 2011 respectively. He worked briefly as a Graduate Engineering Associate at Central Power Research Institute (CPRI) during the year 2011-2013. Currently he is working as a Senior Research Fellow under department of Electrical Engineering at Indian Institute of Technology (BHU). He received the two year fellowship by ministry of human resource and development, Govt. of India during two year masters degree. His current research interest include power converter design and control, power electronics application in power systems and renewable energy.

Comparison on the Performance of Induction Motor Drive using Artificial Intelligent Controllers

P. M. Menghal [1] A. Jaya Laxmi [2]

Abstract–This paper presents an integrated environment for speed control of induction motor (IM) using artificial intelligent controller. The main problem with the conventional fuzzy controllers is that the parameters associated with the membership functions and the rules depend broadly on the intuition of the experts. To overcome this problem, adaptive neuro-fuzzy controller is proposed in this paper.The rapid development of power electronic devices and converter technologies in the past few decades, however, has made possible efficient speed control by varying the supply frequency and voltage, giving rise to various forms of adjustable-speed induction motor drives. The integrated environment allows users to compare simulation results between classical and artificial intelligent controllers. The fuzzy logic controller, artificial neural network and ANFIS controllers are also introduced to the system for keeping the motor speed to be constant when the load varies. The comparison between conventional PI, fuzzy controller, ANN and adaptive neuro-fuzzy controller based dynamic performance of induction motor drive has been presented. Adaptive neuro-fuzzy based control of induction motor will prove to be more reliable than other control methods. The performance of the Induction motor drive has been analyzed for no, constant and variable loads.

Keywords–Proportional integral (PI) controller, fuzzy logic controller (FLC), artificial neural network (ANN), intelligent controller, adaptive-neuro fuzzy inference system (ANFIS).

I. INTRODUCTION

Induction motors (IMs) have been used as the workhorse in industry for a long time due to their easy build, high robustness, and generally satisfactory efficiency [1]. Artificial intelligent controller (AIC) could be the best controller for Induction Motor control. Over the last two decades researchers have been working to apply AIC for induction motor drives [1-6].This is because that AIC possesses advantages as compared to the conventional PI, PID and their adaptive versions. Mostly, it is often difficult to develop an accurate system mathematical model since the unknown and unavoidable parameter variations, and unknown load variation due to disturbances, saturation and variation temperature. Controllers with fixed parameters cannot provide these requirements unless unrealistically high gains are used. Thus, the conventional constant gain controller used in the variable speed induction motor drives become poor when the uncertainties of the drive such as load disturbance, mechanical parameter variations and unmodelled dynamics in practical applications. Therefore control strategy must be adaptive and robust. As a result several control strategies have been developed for induction motor drives in last two decades. This paper presents the speed control scheme of scalar controlled induction motor drive in open loop and closed loop mode, involves decoupling of the speed and reference speed into torque and flux producing components. Fuzzy logic, artificial neural network and adaptive neuro-fuzzy controller (ANFIS) based control schemes have been simulated. The performance of fuzzy logic, artificial neural network and adaptive neuro-fuzzy controller (ANFIS) based controllers is compared with that of the conventional proportional integral controller in open loop and closed loop. The dynamic performance of the induction motor drive has been analyzed for constant and variable loads. Fig.1 and Fig.2 shows the proposed control scheme for an induction motor in open loop and closed loop [9-12].

The paper first received 17 July 14 and in revised form 27 Dec 2014.
Digital Ref: APEJ_2014-07-0444

[1] Faculty of Degree Engineering, Military College of Electronics & Mechanical Engineering, Secunderabad, 500 015, Telangana. Research Scholar, EEE Dept., Jawaharlal Nehru Technological University, Anantapur-515002, Andhra Pradesh, India.
Email: prashant_menghal@yahoo.co.in

[2] Dept. of EEE & Coordinator, Centre for Energy Studies, Jawaharlal Nehru Technological University Hyderabad College of Engineering, JNTUH, Kukatpally, Hyderabad-500085, Telangana, India. Email:ajl1994@yahoo.co.in

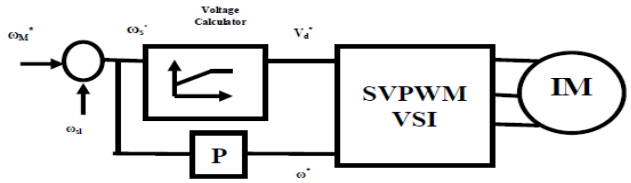

(a) Open loop v/f control.

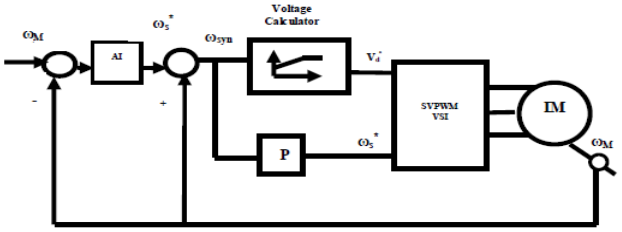

(b) Closed v/f control.

Fig.1: Basic v/f control of induction motor.

Scalar control method is widely used in industries due to its simple structure characterized by low steady-state error. Proportional integral (PI) controllers are commonly used in scalar speed control of induction motors in addition to AI controllers. A mathematical model of the real plant is required for the controller design with conventional methods. The difficulty of identifying the accurate parameters for a complex nonlinear and time-varying nature of real plants may render, in many cases, the fine tuning of parameters which is time consuming. PI controllers are very much sensitive to parameter variations inherent in real plant operations. The gain equation for PI controller

$$T = K_p e + K_i \int e dt$$

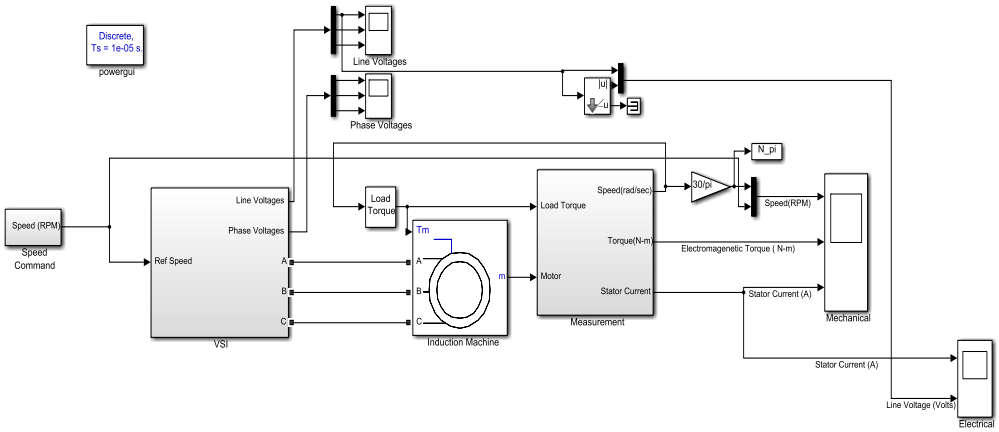

(a) Open loop control.

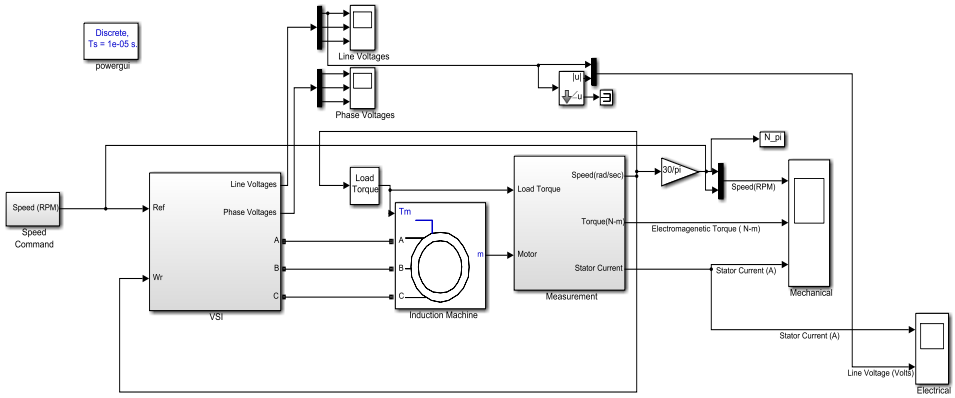

(b) Closed loop control.

Fig.2: Simulated induction motor model with PI controller.

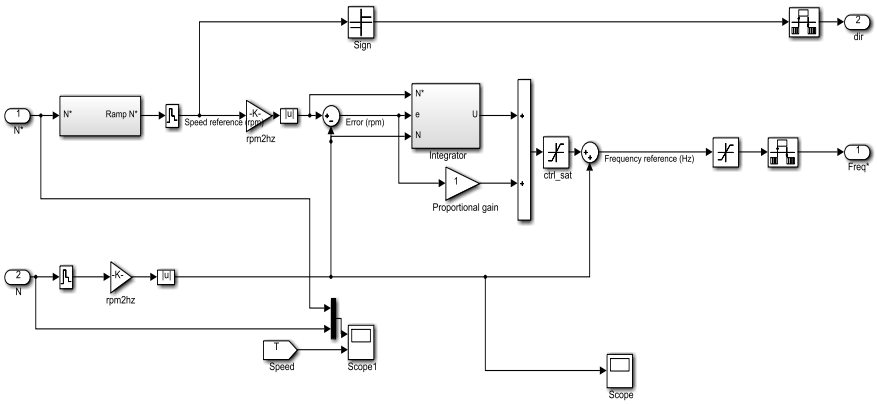

Fig. 3: Structure of PI controller.

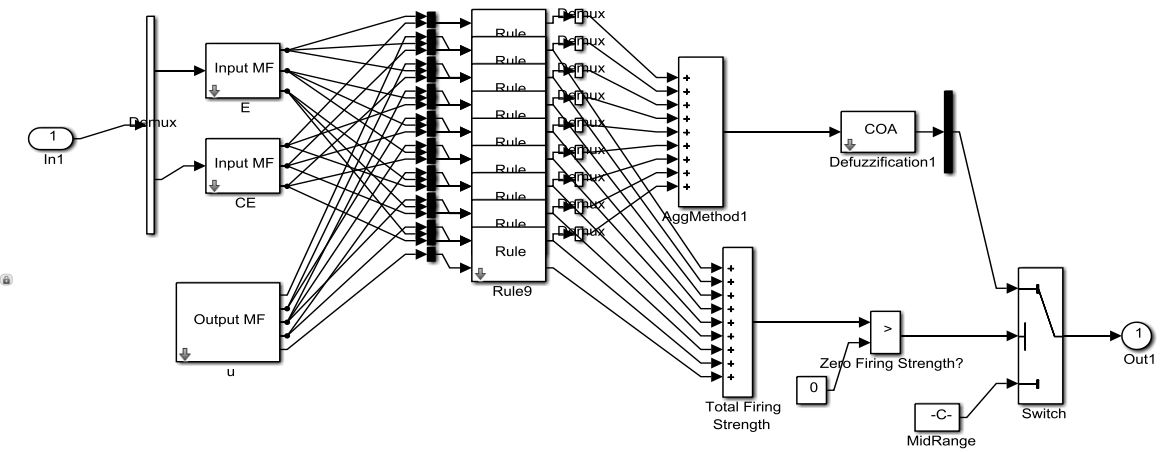

Fig. 4: Structure of fuzzy controller.

The output of the PI controller is updated by updating the PI controller gains (K_p and K_i) based on the control law in the presence of parameter variation and drive nonlinearity. The use of PI controllers for speed control of induction machine drives is characterized by an overshoot during tracking mode and a poor load disturbance rejection. This is mainly caused by the fact that the complexity of the system does not allow the gains of the PI controller to exceed a certain low value. If the gains of the controller exceed a certain value, the variations in the command torque controller gains are very high. The motor reaches the reference speed rapidly and without overshoot, step commands are tracked with almost zero steady state error and no overshoot, load disturbances are rapidly rejected and variations of some of the motor parameters are fairly well dealt, which becomes too high and will destabilize the system. To overcome this problem, we propose the use of a limiter ahead of the PI controller [11]. This limiter causes the speed error to be maintained within the saturation limits. Fig.3 shows the structure of PI controller.

II. Artificial Intelligent Controller

Despite the great efforts devoted to induction motor control, many of the theoretical results cannot be directly applied to practical systems. Intelligent control techniques are generally classified as expert system control, fuzzy-logic control, neural-network control and genetic algorithm. Various artificial intelligent controllers are as follows:

(a) Fuzzy Logic Controller: The speed of induction motor is adjusted by the fuzzy controller. In Table-I, the fuzzy rules decision implemented into the controller are given. The conventional simulated induction motor model as shown in Fig. 2 is modified by adding fuzzy controller and is shown in Fig. 4. Speed output terminal of induction motor is applied as an input to fuzzy controller, and in the initial start of induction motor the error is maximum, so according to fuzzy rules FC produces a crisp value. Then this value will change the frequency of sine wave in the speed controller. The sine wave is then compared with triangular wave to generate the firing signals of IGBTs in the PWM inverters. The frequency of these firing signals also gradually changes, thus increasing the frequency of applied voltage to induction motor [12,14].

As discussed earlier, the crisp value obtained from fuzzy logic controller is used to change the frequency of gating signals of PWM inverter. Thus the output AC signals obtained will be variable frequency sine waves. The sine wave is generated with amplitude, phase and frequency which are supplied through a GUI. Then the clock signal which is sampling time of simulation is divided by crisp value which is obtained from FLC. So by placing three sine waves with different phases, one can compare them with triangular wave and generate necessary gating signals of PWM inverter. So at the first sampling point the speed is zero and error is maximum. Then whatever the speed rises, the error will decrease, and the crisp value obtained from FLC will increase. So, the frequency of sine wave will decrease which will cause IGBTs switched ON and OFF faster. It will increase the AC supply frequency, and the motor will speed up. The inputs to these blocks are the gating signals which are produced in speed controller block. The firing signals are applied to IGBT gates that will turn ON and OFF the IGBTs.

Table I: Fuzzy rule decision.

e \ Δ_e	P	Z	N
P	P	P	Z
Z	P	Z	N
N	Z	N	N

(b) Artificial Neural Network (ANN): One of the most important features of Artificial Neural Networks (ANN) is their ability to learn and improve their operation using a neural network training data[7-8]. The basic element of an ANN is the neuron which has a summer and an activation function. The mathematical model of a neuron is given by:

$$y = \phi \sum_{j=1}^{N} w_j x_j + b \tag{1}$$

where (x_1, x_2... x_N) are the input signals of the neuron, (w_1, w_2,... w_N) are their corresponding weights and b is bias parameter, ϕ is a tangent sigmoid function and y is the output signal of the neuron. The ANN can be trained by a learning algorithm which performs the adaptation of weights of the network iteratively until the error between target vectors and the output of the ANN is less than a predefined threshold. The most popular supervised learning algorithm is back- propagation, which consists of a forward and backward action. In the forward step, the free parameters of the network are fixed, and the input signals are propagated throughout the network from the first layer to the last layer. In the forward phase, we compute a mean square error.

$$E(k) = \frac{1}{N} \sum_{i=1}^{N} ((d_i(k) - y_i(k))^2 \tag{2}$$

where d_i is the desired response, y_i is the actual output produced by the network in response to the input xi, k is the iteration number and N is the number of input-output training data. The second step of the backward phase, the error signal $E(k)$ is propagated throughout the network in the backward direction in order to perform adjustments upon the free parameters of the network in order to decrease the error $E(k)$ in a statistical sense. The weights associated with the output layer of the network are therefore updated using the following formula:

$$w_{ji}(k+1) = w_{ji}(k) - \eta \frac{\partial E(k)}{\partial w_{ji}(k)} \tag{3}$$

where w_{ji} is the weight connecting the j^{th} neuron of the output layer to the i^{th} neuron of the previous layer, η is the constant learning rate. The objective of this neural network controller (NNC) is to develop a back propagation algorithm such that the output of the neural network speed observer can track the target one. Fig. 5 depicts the network structure of the NNC, which indicates that the neural network has three layered network structure. The first is formed with five neuron inputs $\Delta(\omega_{ANN}(K+1))$, $\Delta(\omega_{ANN}(K))$, ω_{ANN}, $\omega_S(K-1)$, $\Delta(\omega_S(K-2))$. The second layer consists of five neurons. The last one contains one neuron to give the command variation $\Delta(\omega_S(K))$. The aim of the proposed NNC is to compute the command variation based on the future output variation $\Delta(\omega_{ANN}(K+1))$. Hence, with this structure, a predictive control with integrator has

been realised. At time k, the neural network computes the command variation based on the output at time *(k+1)*, while the later isn't defined at this time. In this case, it is assumed that $\omega_{ANN}(K+1) \equiv \omega_{ANN}(K)$.The control law is deduced using the recurrent equation given by,

$$\omega_s(k) = \omega_s(k-1) + G\Delta(\omega_s(k)) \quad (4)$$

These terms are considered as disturbances and are cancelled by using the proposed decoupling method. If the decoupling method is implemented, the flux component equations become

$$\Phi_{dr} = G(s)V_{ds}$$
$$\Phi_{qr} = G(s)V_{qs}$$

Large values of η may accelerate the ANN learning and consequently fast convergence but may cause oscillations in the network output, whereas low values will cause slow convergence. Therefore, the value of η has to be chosen

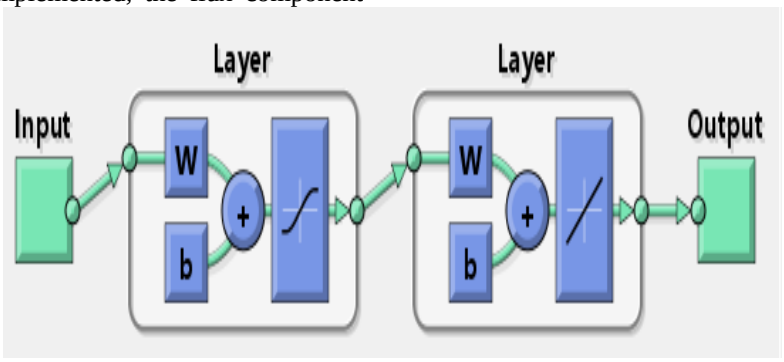

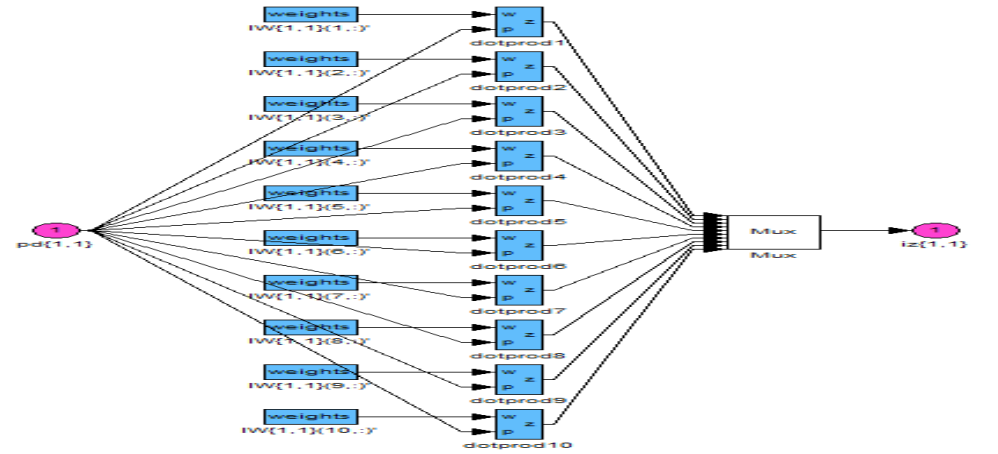

Fig. 5: Structure of neural network controller.

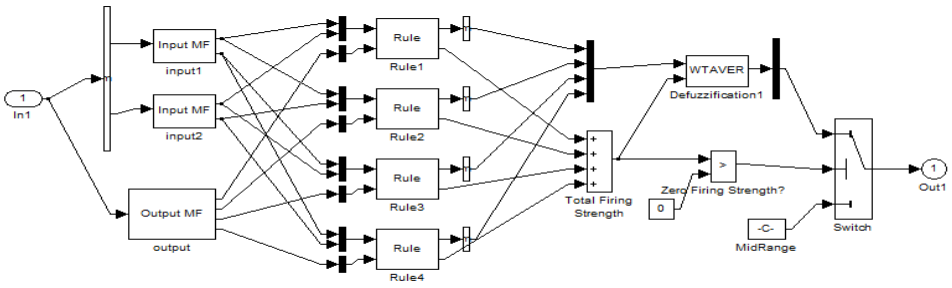

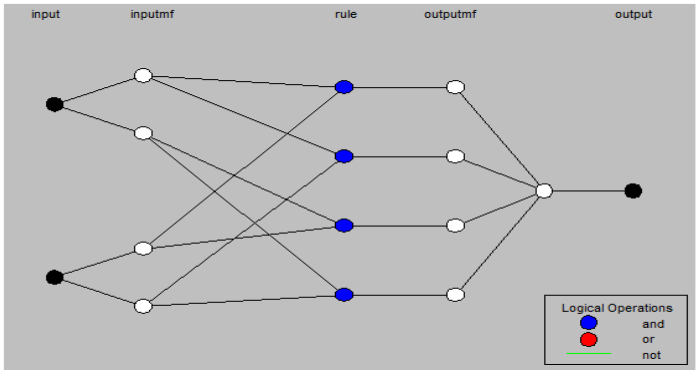

Fig. 6: Structure of adaptive neuro-fuzzy model.

carefully to avoid instability. The proposed neural network controller is shown in Fig. 5 [14-15].

(c) Adaptive Neuro-Fuzzy Controller (ANFIS): AC motor drives are used in multitude of industrial and process applications requiring high performances. In high performance drive systems, the motor speed should closely follow a specified reference trajectory regardless of any load disturbances and any model uncertainties. In the designing of a controller, the main criteria is the controllability of torque in an induction motor with good transient and steady state responses. With certain drawbacks, PI controller is able to achieve these characteristics. The main drawbacks are (i) The gains cannot be increased beyond certain limit. (ii) Non-linearity is introduced, making the system more complex for analysis. With the advent of artificial intelligent techniques, these drawbacks can be mitigated. One such technique is the use of fuzzy logic in the design of controller either independently or in hybrid with PI controller. Adaptive neuro-fuzzy inference system (ANFIS) replaces the draw-backs of fuzzy logic control and artificial neural network. Adaptive neuro-fuzzy combines the learning power of neural network with knowledge representation of fuzzy logic. Neuro-fuzzy techniques have emerged from the fusion of artificial neural networks (ANN) and fuzzy inference systems (FIS) and have become popular for solving the real world problems. A neuro-fuzzy system is based on a fuzzy system which is trained by a learning algorithm derived from neural network theory. There are several methods to integrate ANN and FIS and very often the choice depends on the applications. In this paper, the inputs will be $e(k)$ and $\Delta e(k)$[12]. Fig.6 shows the overall structure of adaptive neuro-fuzzy model.

III. Comparison on Performance Assessment of Artificial Intelligent Controller based Induction Motor Drives

A complete simulation model for scalar v/f controlled induction motor drive incorporating PI, fuzzy logic controller, neural network controller and ANFIS is developed in open loop and closed loop mode. v/f control of induction motor drive with fuzzy controller is designed by proper adjustments of membership functions, neural network controller is designed by adjusting the weights and ANFIS is developed on a fuzzy system which is trained by a learning algorithm derived from neural network theory in order to get simulated results.

The performance of the artificial intelligent based induction motor drive is investigated at different operating conditions. In order to prove the superiority of the ANFIS, a comparison is made with the response of conventional PI, FL and neural network based induction motor drive. The parameters of the induction motor considered in this study are summarized in Appendix A. The performances of the scalar controlled induction motor with all intelligent controllers are presented at constant load and variable load in open and closed loop mode. The dynamic behaviours of the PI controller, FLC controller, neural network controller and ANFIS controller are shown in Fig.7 to Fig. 24 at no load, constant and variable load conditions in open loop and closed loop mode respectively.

(i) At no load condition:

Fig.7 and Fig.16 show the torque speed characteristics of different AI controllers at no load in open and closed loop model. From the characteristics it is observed that the peak overshoot for ANFIS is less as compared to PI, FL and ANN. From the Fig.10, Fig. 13, Fig. 19 and Fig. 22, it is observed that with ANFIS, the torque and speed reaches its steady state value faster as compared to other AI controllers.

(ii)At constant load conditions: 10Nm

A drive with PI controller has a peak overshoot, but in case of fuzzy controller, neural network controller and ANFIS controller, it is eliminated as shown in Fig. 11 and Fig.20 when sudden load of 10Nm is applied to the motor. The PI controller is tuned at rated conditions in order to make a fair comparison. Fig. 8, Fig.11, Fig.14, Fig. 17, Fig. 20 and Fig.23 shows the simulated performance of the drive at starting, with conventional PI, FL, Neural and ANFIS based drive systems, in open loop and closed loop mode respectively. Although the PI controller is tuned by trial and error to give an optimum response at this rated condition, the ANFIS controller yields better performance in terms of faster response time and lower starting current. It is worth mentioning here that the performance obtained by the proposed AI controller is faster than the PI controller, i.e. it achieves the steady state condition faster than the PI controller.

iii)At variable load conditions: 30Nm at 1.5sec

Drive with PI controller speed response has small peak at 0.6 sec, but in case of fuzzy controller, neural network controller and ANFIS controller speed response, it is quick and smooth response which is shown in Fig.9, Fig.12 and Fig. 15, Fig. 18, Fig. 21, Fig. 24. Fig. 15 and Fig. 24 shows the speed response for step change in the load torque using the PI, fuzzy, neural and ANFIS controller, respectively. The motor starts from standstill at load torque = 0 Nm and at t =1.5sec, a sudden full load of 30 Nm is applied to the system, then it is controlled by fuzzy, neural and ANFIS controller. Since the time taken by the PI control system to achieve steady state is much higher than fuzzy, neural and ANFIS controlled system, the step change in load torque is applied at t = 3 Sec. The motor speed follows its reference with zero steady-state error and a fast response using a fuzzy controller, neural and ANFIS. On the other hand, the PI controller shows steady-state error with a high starting current. It is to be noted that the speed response is affected by the load conditions. This is the drawback of a PI controller with varying operating conditions. It is to be noted that the neuro controller and ANFIS gives better responses in terms of overshoot, steady-state error and fast response when compared with PI and fuzzy. These figures also show that the neuro and ANFIS controller based drive system can handle the sudden increase in command speed quickly without overshoot, under- shoot, and steady-state error, whereas the PI and fuzzy controller-based drive system has steady-state error and the response is not as fast as compared to neural network and ANFIS. Thus, the proposed ANFIS based drive has been found superior to the conventional PI-controller, FLC, and ANFIS based system.

Open Loop: Simulation Results

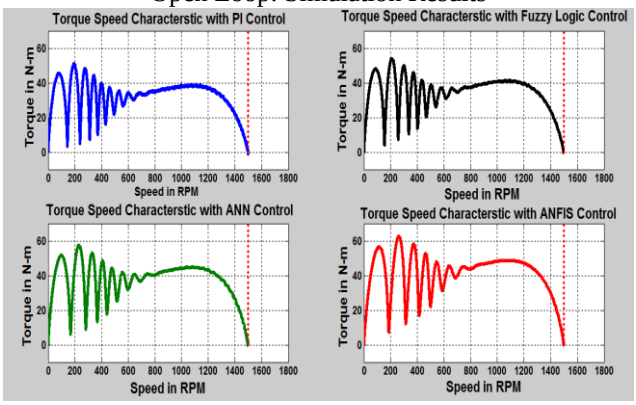

Fig. 7: Torque-speed characteristics: AI controllers at no load.

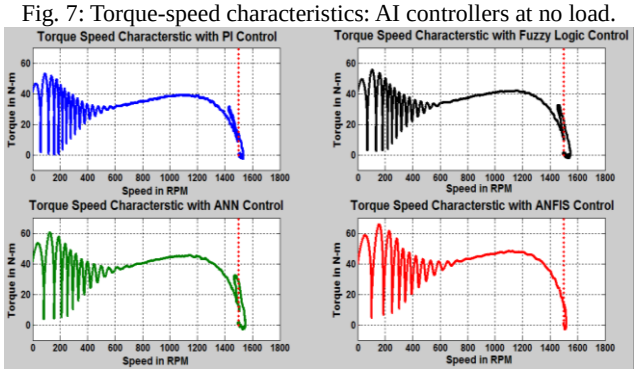

Fig. 8: Torque-speed characteristics: AI controllers at const. load.

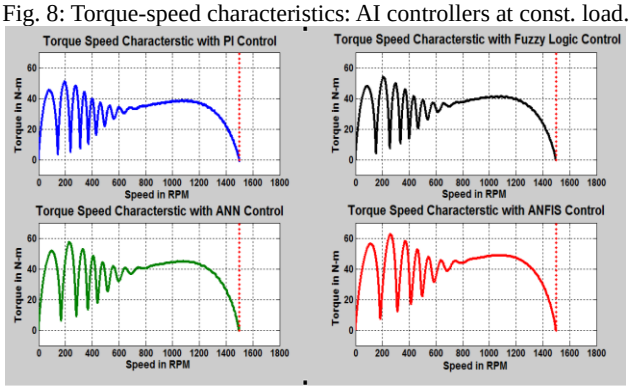

Fig. 9: Torque-speed characteristics: AI controllers at variable load.

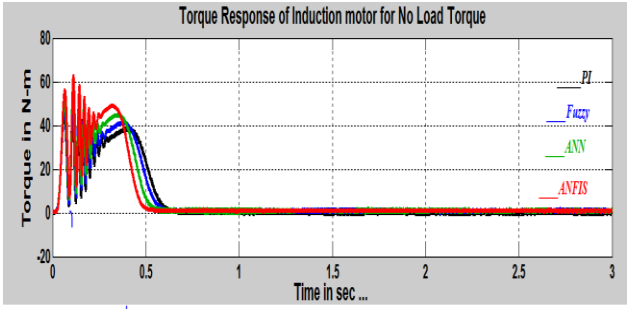

Fig. 10: Torque responses: AI Controllers at no load.

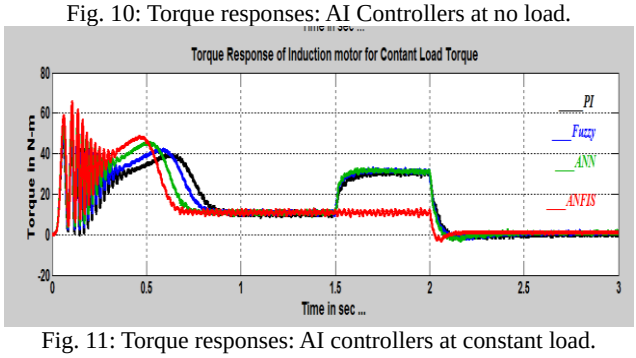

Fig. 11: Torque responses: AI controllers at constant load.

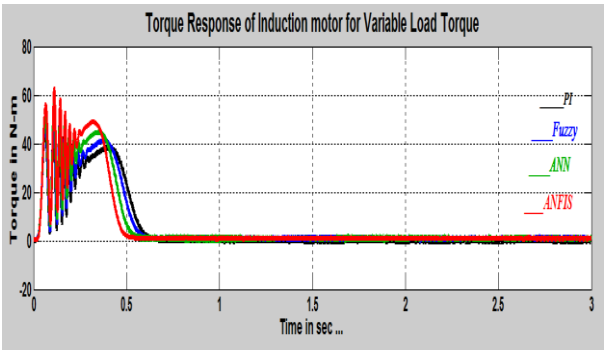

Fig. 12: Torque responses: AI controllers at variable load.

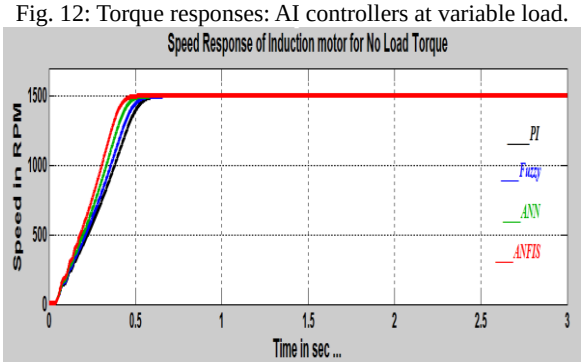

Fig. 13: Speed responses: AI controllers at no load.

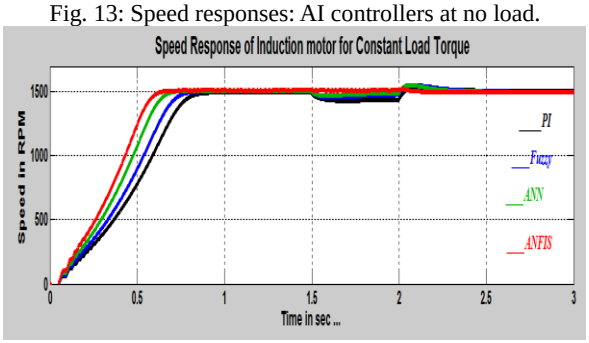

Fig. 14: Speed responses: AI controllers at const. load.

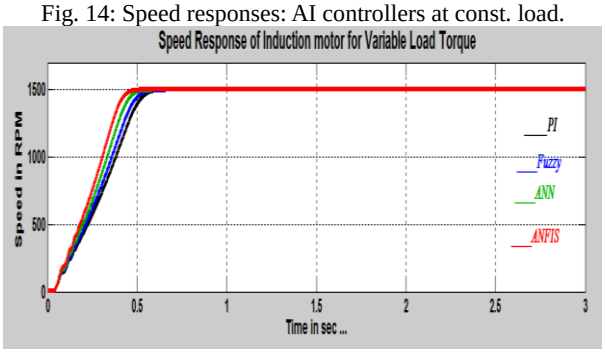

Fig. 15: Speed responses: AI controllers at variable load.

Closed Loop: Simulation Results

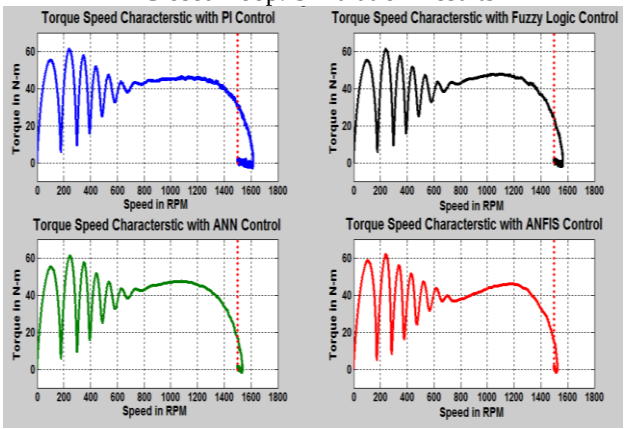

Fig.16: Torque-speed characteristics: AI controllers at no load.

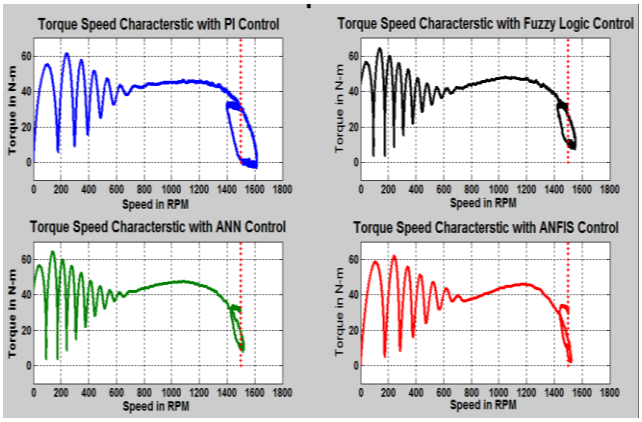

Fig.17: Torque-speed characteristics: AI controllers at const. load.

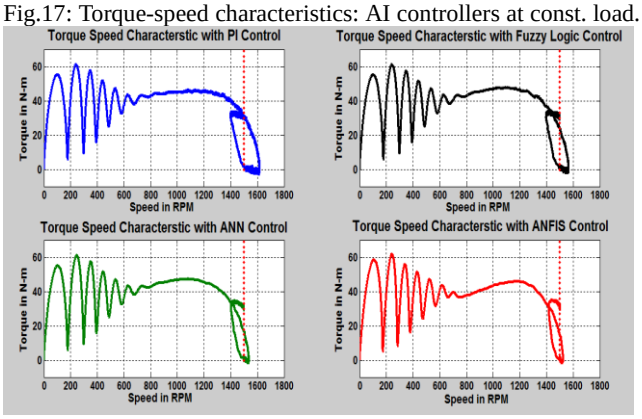

Fig.18: Torque-speed characteristics: AI controllers at variable load.

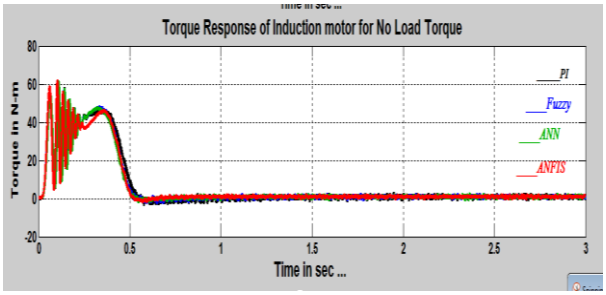

Fig. 19: Torque responses: AI controllers at no load.

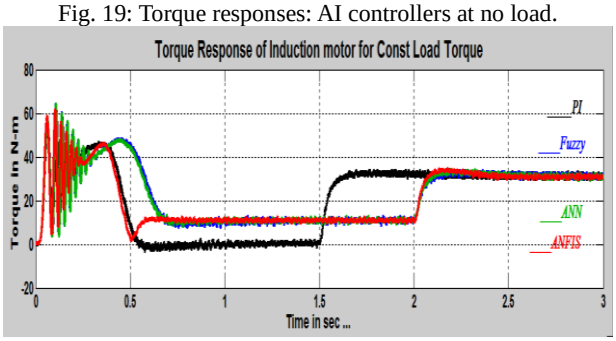

Fig. 20: Torque responses: AI Controllers at constant load.

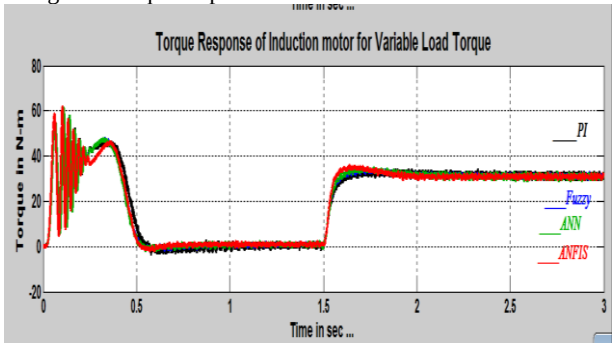

Fig. 21: Torque responses: AI controllers at variable load.

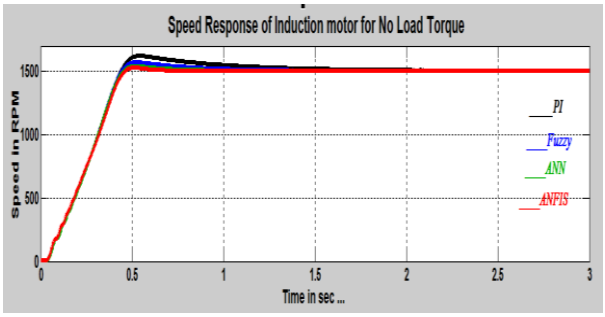

Fig. 22: Speed responses: AI controllers at no load.

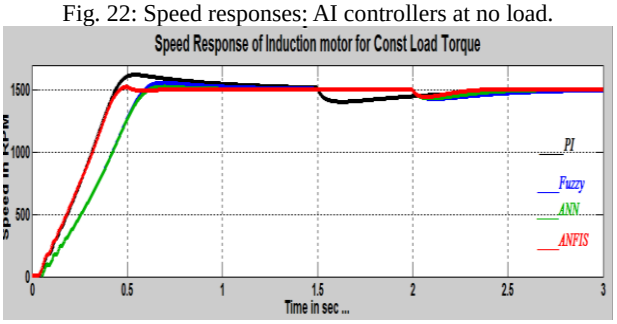

Fig. 23: Speed responses: AI controllers at const. load.

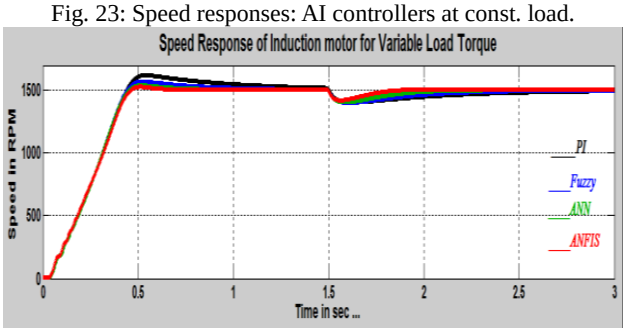

Fig. 24: Speed responses: AI Controllers at variable load.

VI. Conclusion

In this paper, simulation results of the induction motor are presented in conventional PI, FL, ANN and ANFIS. As it is apparent from the speed curves in four models, the fuzzy controller drastically decreases the rise time, in the manner which the frequency of sine waves are changing according to the percentage of error from favorite speed. The frequency of these firing signals also gradually changes, thus increasing the frequency of applied voltage to induction motor. According to the direct relation of induction motor speed and frequency of supplied voltage, the speed also will increase. With results obtained from simulation, it is clear that for the same operation condition of induction motor, fuzzy controller has better performance than the conventional PI controller. By comparing Adaptive neuro-fuzzy model with FL model, it is apparent that by adding learning algorithm to supplied voltage, the speed will also increase. With results obtained from simulation, it is clear that for the same operation condition of induction motor, fuzzy controller has better performance than the conventional PI controller. By comparing Neural network controller with FLC, it is apparent that by adding learning algorithm to the control system will decrease the rising time more than expectation and it proves ANFIS controller has better dynamic performance as compared to NN, FL and conventional PI controller. The comparative results prove that the performance of scalar v/f-control drive with ANFIS controller is superior to that with conventional PI, fuzzy and neural network controller. Thus, by using ANFIS

controller the transient response of induction machine has been improved greatly and the dynamic response of the same has been made faster. For variable loads, when there is a sudden change in load, the ANFIS controller reaches its steady state value faster and there are no overshoots as compared to the PI, Fuzzy and NN controller. This proves the robustness of ANFIS controller.

APPENDIX A

The following parameters of the induction motor are chosen for the simulation studies:

V = 415V	f = 50Hz	Rated Power = 2200 Watts
R_s = 1.115 Ω	R_r = 1.083 Ω	L_s= 0.005974H
L_r= 0.005974H	L_m = 0.2037H	p = 4
J = 0.1kg-m^2	f= 0.005752 Nms	

REFERENCES

[1] K. L. Shi, T. F. Chan, Y. K. Wong and S. L. Ho, "Modeling and simulation of the three phase induction motor using SIMULINK," *Int.J. Elect. Engg. Educ.*, vol. 36, pp. 163-172, 1999.

[2] T. F. Chan and K. Shi, Applied intelligent control of induction motor drives, IEEE Willey Press, First edition, 2011.

[3] P.C. Krause, Analysis of electrical machinery and drives system, IEEE Willey Press, 2000.

[4] N. Mohan, Advanced electric drives: analysis, control modeling using simulink, MNPERE Publication, 2001.

[5] H. E. Jordan, "Analysis of induction machines in dynamic systems," *IEEE Trans. on Power Apparatus and Systems* vol.84, no. 11, pp. 1080-1088, November 1965.

[6] H. C. Stanley, "An analysis of the induction machine," *AIEE Trans*, vol-57, pp. 751-757, 1938.

[7] P. M. Menghal and A. Jaya Laxmi, "Scalar control of an induction motor using artificial intelligent controller," IEEE International Conference Power, Automation and Communication (INPAC2014), pp. 60-65, Oct. 2014.

[8] P. M. Menghal and A. Jaya Laxmi, " Dynamic simulation of induction motor drive using neuro controller," *International Journal on Recent Trends in Engineering & Technology*, vol. 10, no. 1, pp. 44-58, Jan. 2014.

[9] P. M. Menghal and A. Jaya Laxmi, "Neural network based dynamic performance of induction motor," Springer Proceeding Advances in Intelligent Systems and Computing (AISC), vol.259, pp. 539-552, Apr. 2014.

[10] P. M. Menghal and A. Jaya Laxmi, "Application of artificial intelligence controller for dynamic simulation of induction motor drives," *Asian Power Electronics Journal*, vol. 7, no. 1, pp. 23-29, Sep. 2013.

[11] P. M. Menghal, A. Jaya Laxmi and N. Mukhesh, "Dynamic simulation of induction motor drive using artificial intelligent controller," IEEE International Conference on Control, Instrumentation, Energy & Communication (CIEC14), pp. 301-305, Jan. 2014.

[12] P. M. Menghal and A. Jaya Laxmi, "Adaptive neuro-fuzzy based dynamic simulation of induction motor drives," IEEE International Conference Fuzzy Systems, pp. 1-8, 7-10 July 2013.

[13] P. M. Menghal and A. Jaya Laxmi, "Neural network based dynamic simulation of induction motor drive," IEEE International Conference on Power, Energy and Control (ICPEC-13), pp. 566-571, 6-8 Feb 2013.

[14] P. M. Menghal and A. Jaya Laxmi, "Adaptive neuro-fuzzy interference (ANFIS) based simulation of induction motor drive," International Review on Modeling and Simulation (IRMOS), vol. 5, no. 5, pp. 2007-2016, Oct. 2012.

[15] M. N. Uddin and M. Hafeez, "FLC-based DTC scheme to improve the dynamic performance of an IM drive," *IEEE Trans. on Industry Applications*, vol. 48, no. 2, pp. 823-831, Mar/Apr 2012.

[16] Howard E. Jordan, "Analysis of Induction Machines in Dynamic Systems," *IEEE Trans. on Power Apparatus* And Systems Vol. Pas-84, No. 11 November 1965,pp 1080-1088.

[17] M. N. Uddin and H. Wen, "Development of a self-tuned neuro-fuzzy controller for induction motor drives," *IEEE Trans on Industry Application*. vol. 43, no. 4, pp. 1108-1116, July/August. 2007.

[18] M N. Uddin, T. S. Radwan and A. Rahman, "Performance of fuzzy logic based indirect vector control for induction motor drive," *IEEE Trans on industry application*, vol. 38, no.5, pp. 1219-1225, Sept/Oct. 2002.

[19] H. C. Stanley, "An Analysis of the Induction Machine," *AIEE Trans*, vol-57,1938,751-757.

BIOGRAPHIES

P. M. Menghal was born in Khapa (Village), Nagpur (District), Maharashtra India on 7th Feb 1975. He received B.E. degree in Electronics and Power Engineering from Nagpur University, Nagpur in 1998, Master Degree in Control Systems, from Government College of Engineering, Pune, University of Pune, India in 2000 and pursuing Ph.D. at JNT University, Anantapur, Andhra Pradesh. Presently he is working as a Assistant Professor, Faculty of Degree Engineering, Military College of Mechanical Engineering, Secunderabad, Telangana, India.. He is a Member of IEEE, Institute of Engineers (M.I.E.), Kolkata India, Indian Society of Technical Education(M.I.S.T.E.), IETE, Indian Science Congress and System Society of India (S.S.I He has 20 International and National Journals to his credit. He has 25 International and National papers published in various conferences held at India and also abroad. His current research interests are in the areas of Real Time Control system of Electrical Machines, Robotics and Mathematical Modeling and Simulation.

A. Jaya Laxmi was born in Mahaboob Nagar District, Andhra Pradesh, on 07-11-1969. She completed her B.Tech. (EEE) from Osmania University College of Engineering, Hyderabad in 1991, M. Tech.(Power Systems) from REC Warangal, Andhra Pradesh in 1996 and completed Ph.D.(Power Quality) from Jawaharlal Nehru Technological University College of Engineering, Hyderabad in 2007. She has five years of Industrial experience and 13 years of teaching experience. She has worked as Visiting Faculty at Osmania University College of Engineering, Hyderabad and is presently working as Professor & Coordinator, Centre for Energy Studies, JNTUH College of Engineering, JNTUH, Kukatpally, Hyderabad. She has 40 International Journals to her credit. She has 100 International and National papers published in various conferences held at India and also abroad. Her research interests are Neural Networks, Power Systems & Power Quality. She was awarded "Best Technical Paper Award" for Electrical Engineering in Institution of Electrical Engineers in the year 2006. Dr. A. Jaya Laxmi is a Member of IEEE and IAO, Life Member of System society of India, Fellow of Institution of Electrical Engineers Calcutta (M.I.E) and also Life Member of Indian Society of Technical Education (M.I.S.T.E), MIETE, Indian Science Congress.

Low Voltage DC Distribution System

K. Ding [1], K. W. E. Cheng [2], D.H. Wang [3], Y.M. Ye [4], X.L.Wang [5], J.F.Liu [6]

Abstract–AC distribution is conventional and its future is now under threat with its major competitor DC distribution. Transformer voltage conversion can be replaced completely by DC-DC converter in DC distribution with voltage and current regulation. DC energy and energy saving as the distribution match well with the recent technology in renewables, energy storage, computer and control electronics, modern lightings and electric mobility which are all DC based. Using DC, the AC-DC and DC-AC conversions will no longer be needed. The higher processing efficiency, simple control in power quality, easy voltage source connection and material reduction are the obvious advantages. The paper discusses the recent development of DC distribution and its technology. The work in voltage level, soft-switching, safety and protection are the area of recent development. Power Electronics is a driving force to realize this future power distribution. Analyses on the voltage and efficiency are also complemented with the description. It is expected that the DC distribution demonstrates a power innovation in the world and open a new chapter for energy saving and power utilization.

Keywords–DC distribution, AC distribution, energy storage, DC-Dc converter, inverter

I. INTRODUCTION

AC distribution has been used for more than a century. Today most of the home, office and industrial appliances or equipment are using AC. The AC distribution allows simple voltage conversion using conversion transformer. Therefore it is still being used widely everywhere [1- 6]. There are a number of disadvantages using AC distribution. The voltage conversion uses power transformer that is based on silicon iron core. They operate under low frequency which is 50Hz. The overall size is large and it needs a lot of materials. The size of the associated components are also many. The AC distribution also suffers from AC loss. Therefore the cross-section of the AC cable is usually larger than DC cable. The harmonic current, power factor and many power quality problems exist in the AC system. It also imposes drawbacks in using the AC system [7-13]. The more important issue is incompatible with the existing technologies. Today almost all the electrical and electronics systems need only DC power [14-19]. This includes the lighting – all LEDs and electronic ballast,; motor driver – all uses DC powered inverters; Entertainment – All amplifier and AV equipment are DC operated; Energy storage – Battery and super-capacitor are DC operated[20]; Renewable energy – Solar panel is DC, wind generator can directly output DC[21-29]; Control and computer- All control electronics and computers are DC operated [30-36]. Power electronics DC conversion technology has been developed and used in DC distribution system extensionally [37-41]. Many apparatus sets are of structure as shown in Fig 1. There is a rectifier that converts AC into DC. The resultant DC of the rectifier is then converted to other DC voltages for different electronic circuits or electrical units. If DC is used directly, the rectifier sub-circuit can be eliminated. The materials can be reduced and the efficiency can be increased. Table I summaries the equipment using DC.

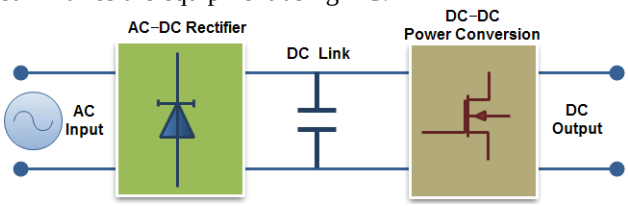

Fig.1: A typical structure of the power supply of an apparatus or equipment.

Table 1: Summary of the appliances using DC

Catalog	Applications
Consumer products	Amplifier, Television set
	Personnel computer
	Blender
	Fans
	Fluorescent lamps and its electronic ballast
	Compact fluorescent lamps and its electronic ballast
	Mobile phone, Home apparatus Charger
	Microwave oven, Induction cooker
Buildings	Ventilation
	Lift, Escalator
	Pump
	UPS, Voltage dip restorer
	VAR compensator, high frequency
	Lighting, LED
Automotive	Traction and train
	Battery charger
	Motion control
Industrial	Motor drives
	Sewing machines
	Pump
	Seawater water maker
	Electric plating
Medical	Wheel-chair, robot
	Functional electrical stimulator (FES)
	Most medical monitoring systems
	MRI

It can be seen that Table 1 cover most of the common electrical and electronic system. Most of them can actually DC connected or directly driven by DC.

The paper first received 1 Aug 2014, in revised from 15 Dec 2014
Digital Ref: APEJ_2014-11-0462
[1,2,3,4,5,6] Department of Electrical Engineering, The Hong Kong Polytechnic University, Hong Kong, China.
E-mail: [1]eekding@polyu.edu.hk, [2]eeecheng@polyu.edu.hk, [3]eedhwang@polyu.edu.hk,[4] yuanmao.ye@connect.polyu.hk, [5]xiaolinee.wang@connect.polyu.hk, [6]jf.liu@connect.polyu.hk

Table 2: Units used AC or DC

Units uses AC or DC	In the future
Incandescent light bulb	Replaced by compact fluorescent lamp, can use DC directly
Constant speed motor such as fans,	Replaced by inverter drives.
Thermal units of filament	Can use DC directly
Simple pump or motor such as aquarium applications	Replaced by DC motors
AC generator	DC generator using DC line power control

Table 3: Comparisons of DC/AC System

	Size Decrement	Energy Saving
Electronic Ballast	30%	5%
Motor Driver	30%	4%
Renewable Energy System	40%	5%
Transmission	50%	2%
Charger	20%	10%
TV/HiFi	10%	10%
Computer	15%	8%
Average	25%	4.5%

Many systems that are originally used in AC can also be used in DC which is shown in Table II. Typical efficiency for the power supply unit for small power electric system is 80% in which the rectifier accounts for 1/3 of the loss. Therefore it will provide 7% of energy saving if DC is used. For high power unit, the rectifier unit accounts for 5%. The saving together with equipment itself and other distribution network, the total loss using DC could be reduced by 50%. Table III summarizes the advantages.

The above discussion clearly shows that DC should be used in the electrical system rather than AC. Presently, all the AC networks are converted to DC firstly before it is connected to the appliances or equipment, either externally or internally. Therefore it is beneficial to use DC to reduce the number of stages of power conversion and reduce the materials used in power conversion, hence to increase the efficiency, simplify the power conversion, improve the reliability, simplify summation or parallel of voltage and load, and simplify the power quality circuit. Today the technology of power electronics is mature. High frequency DC-DC power conversion is simple, low cost, high efficiency and readily available to be used for this duty. All the above can be realized by DC power conversion technology.

II. Structure and DC bus voltage levels

A.DC layer structure

DC distribution power system (DPS) can be an alternative method to deliver the power to the end of the user. The driving force comes from the rapid evolution of power electronic device, the cost, stability, safety and efficiency requirement, the integration and modularize requirement of the system. And the most importance is the emerging need for DC power supply for all electric and electrical products that most of them have power electronics circuits. DC distribution method allows the incorporation of recent improvement in power electronics, and obtains significant improvement in design and manufacturing process. A typical DC distributed power system is shown in Fig. 2. The main structure of the DPS contains power sources which are commonly parallel connected and delivers power to the intermediate bus, the voltage level in this system is 310V dc and also several load converters to convert the specified voltage to the customer. In Fig. 2, the power sources include renewable resources such as wind power, photovoltaic generation, and also battery backup which power the loads when the two main power sources fail to supply electricity in a short period and a redundancy generator activates when wind power and photovoltaic fail in a long period.

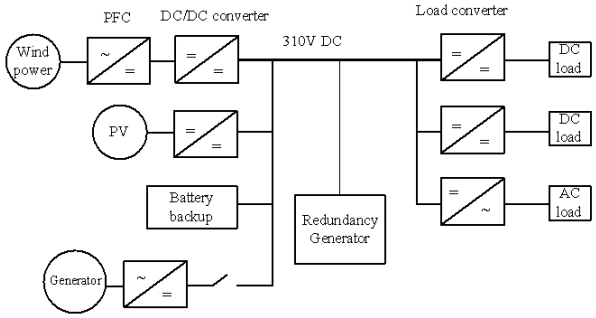

Fig. 2: DC distribution system with renewable sources generation.

The double-layer DC distributed power system employed in this paper is shown in Fig.3. The high voltage DC level is 300V~310V DC and the low voltage DC level is 20V~24V. All the DC buses also have an earth bus for the implementation.

B.DC bus voltage levels

The appropriate DC bus voltage level selection is the key step in the DC distribution system design which has great impact on the performance and characteristic of the entire power system. The DC bus voltage ranges from 12V to 400V in a low voltage distribution system. For most desktop computer system, 12V DC bus is a better choice than the traditional AC bus, which reduces power conversion stage from AC mains to 12V DC voltage while military and aerospace power units have a long history of standardizing on 28V DC. For telecommunication company, the 48V DC has been used for years on the telecommunicate applications powered by 48V DC voltage partly because of the widely available 12V DC batteries. Now, DC has been considered as an alternative system for power distribution or at least a hybrid system which incorporating in parallel existence with AC distribution system since AC power system is still the commonly accepted distribution and still be used for a long time partly due to mature AC standard and regulations. 300V~310 V DC are considered to be economic and effective enough to apply to the existing system and be compatible to the most products in use today. With an agreement on 36 V as the maximum safety voltage that will not create a hazard in China, a nominal voltage of 20V~24V DC has been accepted as the best

compromise between DC/DC conversion efficiency and safety. Therefore, 20V~24V DC bus voltage has been considered as the choice of the voltage level in low voltage distributed power system.

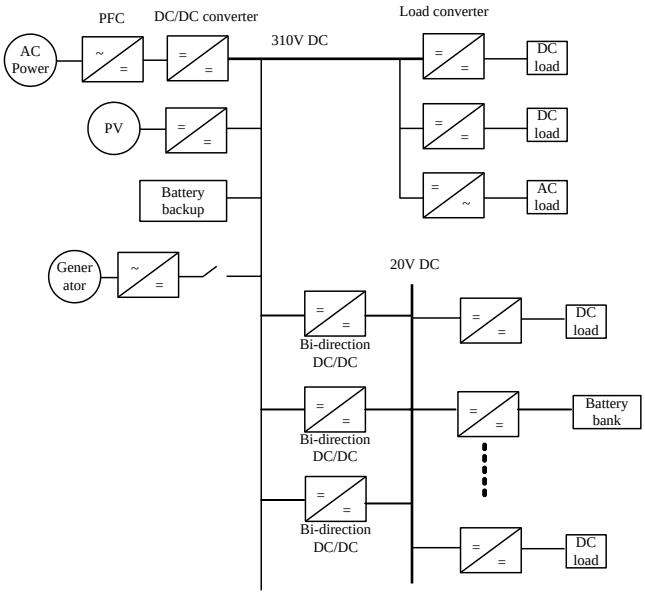

Fig. 3: DC distribution system with double-layer structure.

C. Proposed DC System

The schematic of proposed DC system is shown in Fig. 4. The system includes the power source, AC/DC converters, renewable energy, DC/DC converters, batteries pack and electronics load used in home.

III. Units in DC System

A. Renewable energy system

The recent rapid growth of renewable energy technologies, such as solar photovoltaic and wind turbines, are dramatically changing the nature of transmission, distribution and utilization of electrical energy. Most of storage equipments include batteries and ultra-capacitors that operate on DC voltage. Most renewable energy include solar and wind which have been widely utilized in household, industry and commerce. The electrical energy produced by renewable energy systems like photovoltaic panels is in the form of the DC electrical energy. In effect, despite of the fact that the electrical energy produced by the wind turbines is in the form of AC in certain proportion to the wind speed, this AC energy is converted into the DC energy by its converters. Thus, the DC energy produced by photovoltaic panels and wind turbines have to be converted into AC energy due to the fact that the consumers are all AC. Such a DC/AC conversion brings disadvantages such as the need of a DC/AC converter, the involvement of some harmonics, and the loss of energy in converter stages, special DC link design, the increase in dimension and cost, and degradation of the dynamic response.

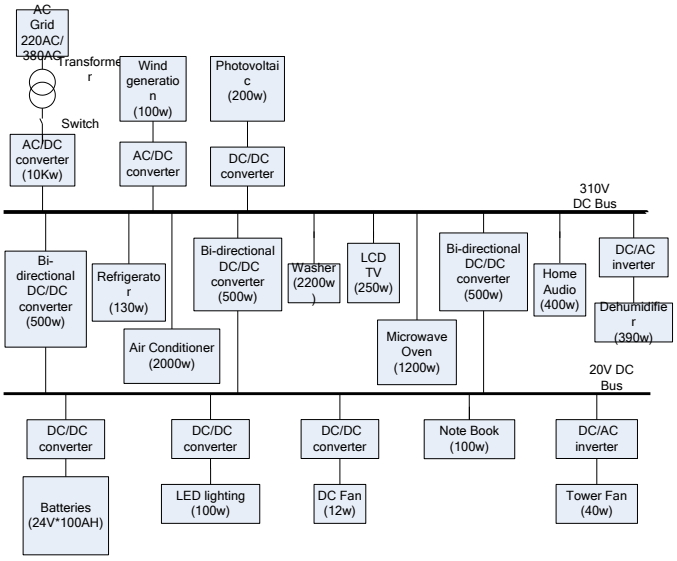

Fig. 4: The schematic of the DC System.

B. DC energy systems

The transmission of the electrical energy from the place of production to the place of consumption comes with the problem of the loss of energy. The transmission of the energy produced by renewable energy systems with the least possible loss is extremely important since these systems are expensive and the power generator may be is discontinuous. In the AC energy system, the power factor gets involved and hence this adversely affects the active power transmitted. Such a problem in power factor and the associated energy loss due to power factor does not exist in DC systems as the power factor is considered to be unity in the DC energy transmission. The energy produced by photovoltaic panels, fuel cells and wind turbines is in the form of DC and thus we can abstain from the above mentioned problems if we use DC loads without the need of DC/AC conversion.

In addition, changing DC to AC is relative expensive and inefficient, while regulating DC or changing AC to DC is both cheap and efficient. DC/AC inverters are quite complex, while DC/DC conversion are relatively simple and mature, and AC/DC rectifiers are extremely simple. Therefore, it is quite easy to import either DC or AC power or even both into a DC energy system but relatively difficult to import DC power into an AC grid.

IV. New challenge of DC system

The switch or breaker should be revisited as the DC condition is different from AC condition. All switching units are examined and new DC switching units are introduced.

A. New Thyristor DC Circuit Breakers with Novel ZCS Technique

DC current is the key concern in DC system. There is no zero crossing point as in the AC system which usually sinusoidally varies with time. Incorrect switching on and off of a DC current will introduce transient incident such as high voltage breakdown. This produces electromagnetic interference, reduces the component age and increases other transient operational risk. The obvious

solution is to use zero-current switching (ZCS) that reduce the switching transient. The following is a new introduced DC switching breaker.

In order to simplify the capacitor self-charging circuit of thyristor DC circuit breakers for low voltage residential and commercial applications, a novel topology is developed as shown in Fig.5. In normal operation state, thyristor T_{main} is turned on to carry current for the load. Meanwhile, the Mosfet S is also turned on to provide the charging path for the capacitor C_r. In the beginning of an interruption process, thyristor T_{aux} is turned on and S is being off. The current of the LC resonant tank increases from zero. The main switch T_{main} will be off when the resonant current increases to the level of the load current. At the end of the process, the auxiliary switch T_{aux} is also turned off when the capacitor C_r is fully charged in opposite polarity and the interruption process is completed.

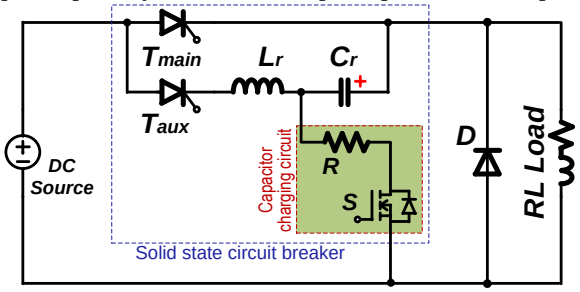

Fig.5: Thyristor DC circuit breaker with simplified self-charging circuit.

Fig 5 gives only a single wire thyristor DC circuit breaker which only has a limited protection as there is still one wire not being off. For complete protection, all electric conductors should be turned off during fault condition. A new four terminal thyristor DC circuit breaker are developed as given in Fig.6. With the proposed unit, faults can be totally isolated from the power source. The positive and negative buses are protected through the two combinations of thyristor switches as seen in the upper rail and lower rail, respectively. However, there is only one capacitor charging circuit required to provide energy for the two capacitors before responding to an interruption command. In order to ensure there are the same amounts of energy pre-charged in the two capacitors, passive balance resistors R_P are employed. It should be noted that the value of R_P is not only far larger than the charging resistor R_S, but also so large that the auxiliary switch T_{aux} could be off automatically at the end of an interruption process. The operation principle of this new circuit breaker is the same as that of one shown in Fig.5, but has extended to the both rails.

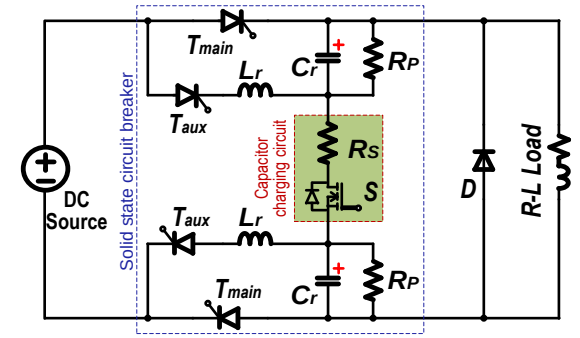

Fig.6: Four-terminal thyristor DC circuit breaker with self-charging circuit.

B. Design of DC RCD

The measurement component of this paper is the single core DC leakage current sensor based on magnetic modulation. The difference with the traditional sensor is that the single core and single coil.

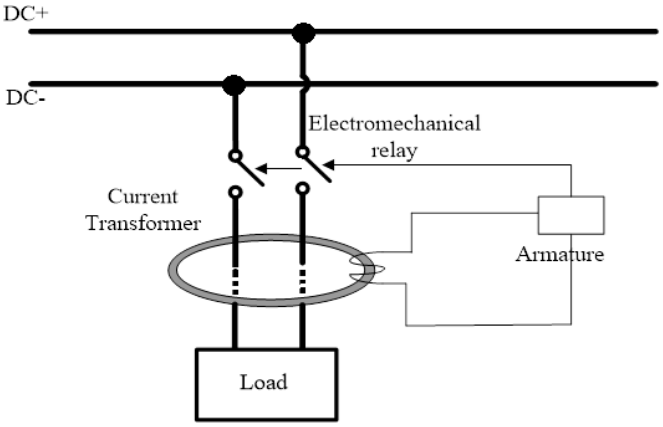

Fig. 7: Connection diagram of RCD in the DC system.

As shown in Fig. 7, the transformer coil is used to detect the leakage current signal through the differential current of the load. The signal received is sent to a signal conditioning circuit, and then processed by the signal conditioning circuitry. A microcontroller is used to provide the decision and identification of the leakage current level for human protection. The RCD DC unit executes the turn-off action, and visual display is implemented to assist the operation. An LED light indicates the working status of the system to achieve a real-time display and DC leakage current self-diagnostic result, and of course provides action and alarm.

C. Effect of DC current on human being

As shown in Fig. 8, the impedance of human being can be divided into internal impedance and impedance of the skin. The internal impedance of the human body is considered as resistive. Its value depends primarily on the current path and the contact area. The impedance of the skin is viewed as a combination of resistances and capacitances. The skin impedance falls as the increased current. The total impedance of the human body is higher for DC.

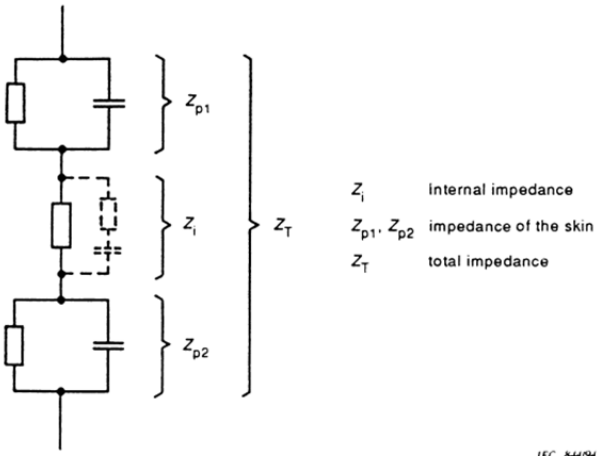

Fig. 8: Impedance of the human body [42].

At the moment of touching voltage, skin impedances are negligible. The initial resistance is approximately equal to the internal impedance of the human body. Therefore, the initial resistance is determined by the current path. The capacitances in the human body are charged as soon as electrical excitation, and the impedance of the human body is close to the addition of internal impedance and skin impedance. The experiments are conducted to measure the DC impedance of human, and the corresponding results are demonstrated in Fig. 9.

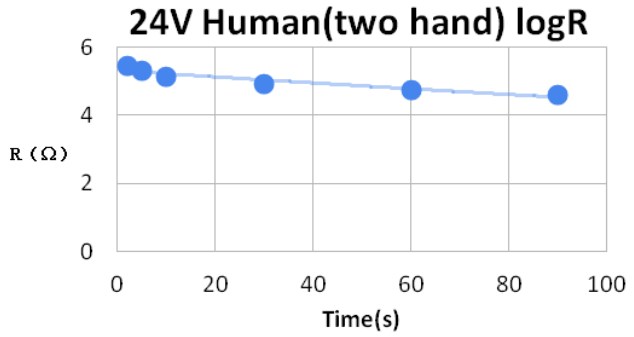

(a)

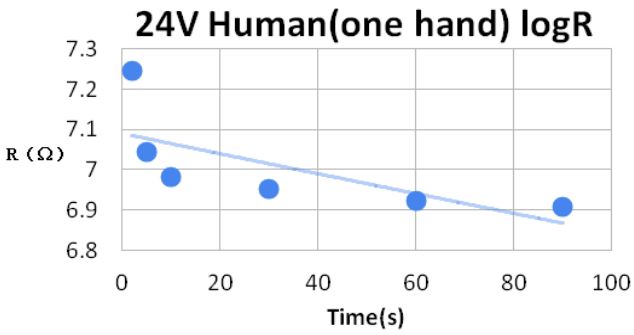

(b)

Fig. 9: DC impedance of human at the given conditions.

The impedances of two hands are shown in Fig. 9a with 24V DC voltage; while the impedances of one hand are shown in Fig. 9b with 24V DC voltage. It can be found that the impedance is decreased along with the time applied duration of DC electric shock.

According to the impedance characteristics of DC current, the raw data processing can be accomplished by wavelet analysis, and the obtained signals are viewed as the input of Neural Network. The compositional structure can avoid the input disturbance to BP Neural Network, and signals preprocessing of wavelet analysis ensures the accuracy and stability. Meanwhile, this structure can fully exert their advantages as the wavelet analysis has high resolution and BP Neural network has nonlinear approximation. The leakage current protection is made intelligent with adaptive identification and high fault tolerance. Since the impedance model is stable and high accurate, the personal electric shock current can be effectively detected with fast response time.

V. The Analysis and Simulation Platform of DC Systems Set Up

A. Simulation System

As shown in Fig. 10, using an ideal voltage source V_S (310V) with a series-connected resistor R_s (1mΩ) as the power source of the whole DC distribution system. In this case, the level of 310V is directly obtained from the power source V_S whereas the level of 20V is converted by a high step-down DC/DC converter.

Considering the load characteristics in the DC distribution system, all different types of loads are replaced by the pure-resistance load with different values. It means just active power is considered here. There are four loads with total power 256W for the lower-voltage bus (20V) while seven loads with the total power 6.78kW on the higher-voltage bus (310V).

Each load is connected to the DC buses through an ideal switch. This switch is just used to start and stop the load operation and there is no power regulation function.

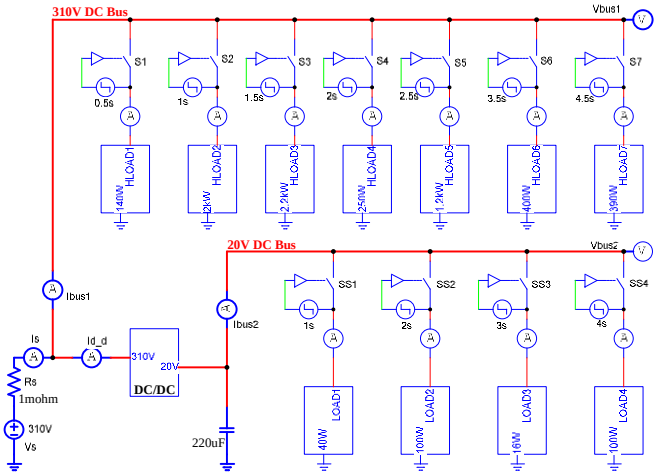

Fig. 10: Simulation System for DC Distribution.

B. Step Loads Response

Step Load means the loads are gradually added to the DC bus and the power source will endure maximum power operation test at the end when all loads run simultaneously. Fig. 11 (a) and 11 (b) provide the start-up sequence of all loads for the higher- and lower-voltage buses, respectively.

When the four loads are connected to the lower-voltage bus step by step, the bus responses including voltage V_{bus2} and current I_{bus2} are obtained as shown in the upper of Fig. 11(c). It shows the bus current increases gradually from zero to maximum value 12.8A whereas the bus voltage remains constant 20V. However, there are small spikes found in the bus voltage when the load is changed suddenly. These voltage spikes could be eliminated or reduced by using the more advanced DC/DC power converter to obtain the lower bus voltage from higher-voltage bus. It also could be optimized by employing an energy storage device with high power density, like super-capacitor.

Similarly, with the seven loads are gradually added to the higher-voltage bus, the bus current I_{bus1} also increases from zero to the maximum 21.9A. As shown in the lower of Fig. 11(c), it could be found there is a slight bus voltage drop with the increase in load. It is actually caused by the internal resistance of the power source, i.e. R_S. In practical, the resistance of wires also will contribute for the voltage

drop. It means the high internal resistance of both source and wires should be avoided in practical DC distribution system.

Additionally, the injection current I_{d_d} from the higher-voltage bus to the lower bus and the total current I_S flowing out of the power source are also obtained as shown in Fig. 11(d).

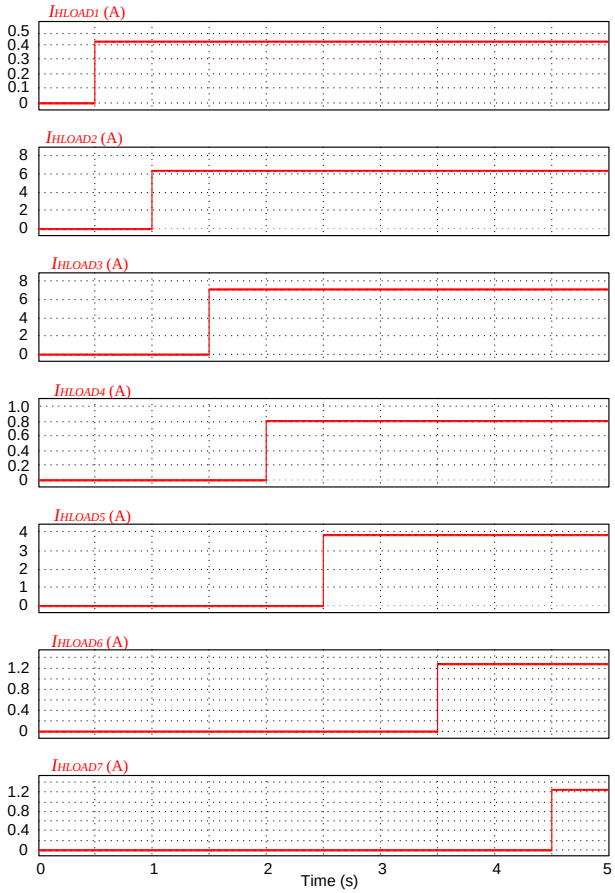

(a) Loads start-up sequence of the higher-voltage bus

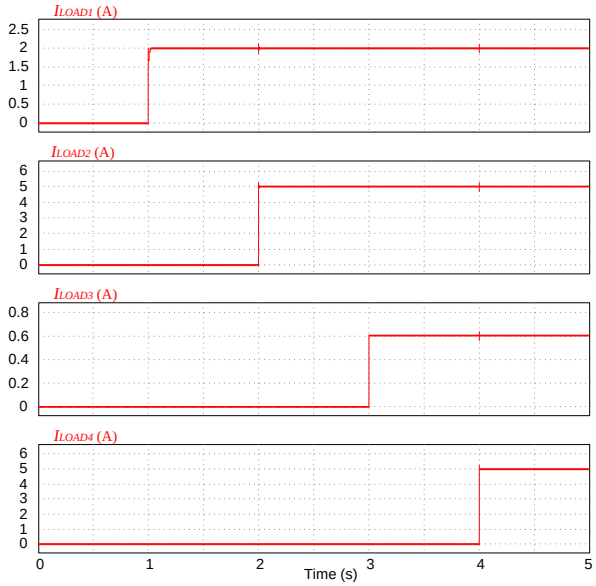

(b) Loads start-up sequence of the lower-voltage bus

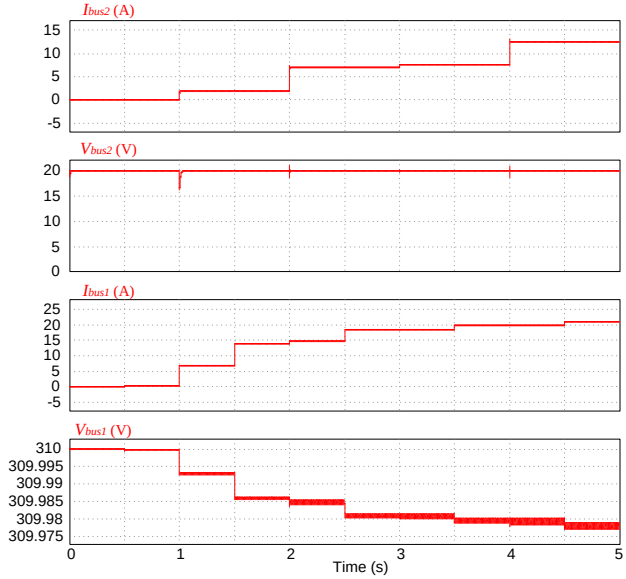

(c) Bus currents and voltages

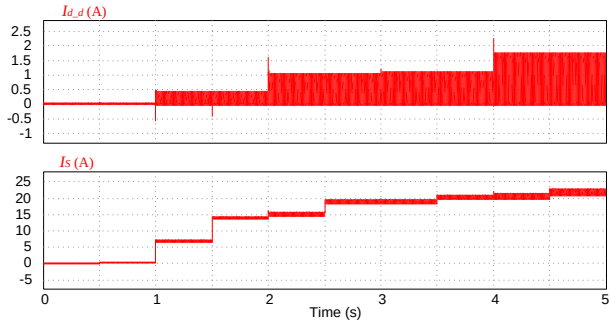

(d) Exchanging current *Id_d* between buses and total input current.

Fig. 11: Simulation results for the dual-level DC distribution system with step loads.

C. Pulse Load Response

Pulse loads sequence is given in Fig. 11(a) of which the upper is for the higher-voltage bus and the lower is for the lower-voltage bus. Each load is connected to the buses just for a short period. It means the DC buses will withstand the impact of frequent load change.

The corresponding bus currents under pulse loads operation are obtained as shown in Fig. 11(b). It depicts that the bus currents fluctuate frequently with loads connected or disconnected from the buses.

The bus voltage response for the pulse load is depicted in Fig. 11(c). For the higher bus voltage V_{bus1}, it also fluctuates with the change of bus current I_{bus1}. This could be still explained as the effect of the internal resistance R_S. In contrast, the lower bus voltage V_{bus2} still remain constant 20V but with small voltage spike when the load is connected or disconnected from the bus. This performance could be also optimized by using the same methods present in the last section. Additionally, the soft-start and soft-stop of loads also benefit the bus voltage spike reduction.

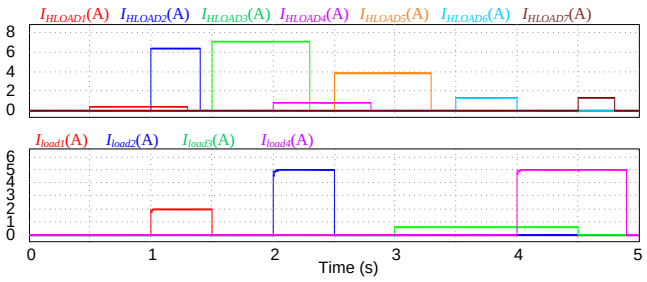

(a) Loads start-up sequence

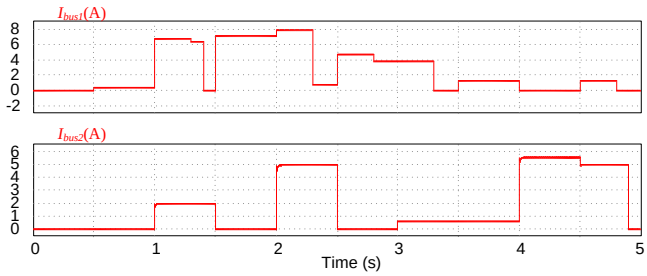

(b) Bus currents

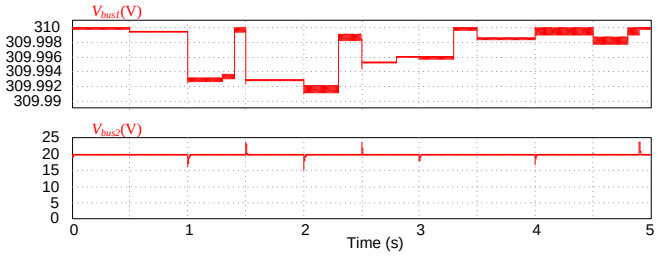

(c) Bus voltages

Fig. 12: Simulation results for the dual-level DC distribution system with pulse loads.

D. Efficiency

The preferred voltage for DC high voltage is examined. The study is using common apparatus for home and office. As shown in Table 4, in the simulation study of higher DC voltage, these selected appliances are typical ones and of course other combination can also be used.

Table 4: Load for higher DC voltage

Load	Rated Power(W)
Refrigerator	140
Air Conditioner	2000
Washer	2200
LCD TV	250
Microwave Oven	1200
Home Audio	400
Dehumidifier	390

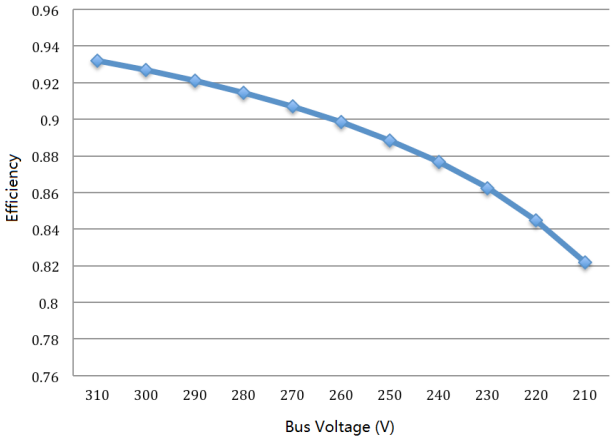

Fig.13: Simulated Efficiency curve for higher DC voltage.

The simulated efficiency curve of higher DC voltage is shown in Fig.13, the efficiency approaches maximum when the voltage reaches over 300V, for the existing electronics appliances, the DC bus voltage is usually smaller than 310V. Also, for single-phase full bridge rectifier, the output voltage is around 310V. If taking into account the input energy from a power source to the DC distribution system, the higher DC voltage needs to be less than 310V. 300V can be used as the preferred voltage in the DC distribution system.

As shown in Table 5, in the simulation study of lower dc voltage, these appliances are used as the load.

Table 5: Load for lower DC voltage

Load	Rated Power(W)
LED lighting	100
Note book	100
DC fan	16
Battery Charger	40

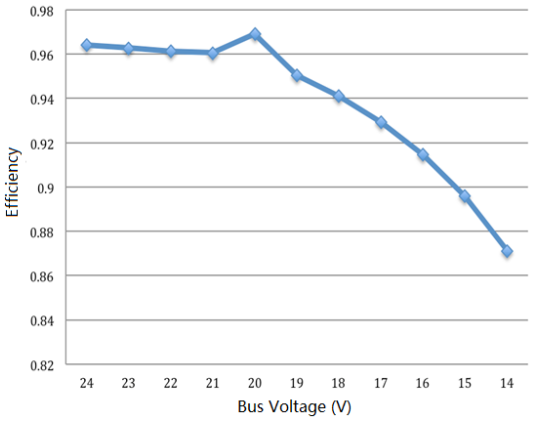

Fig.14: Simulated Efficiency curve for Lower DC voltage.

The simulated efficiency curve of lower DC voltage is shown in Fig.14. The dc bus voltage can be connected to the 20V voltage, so the efficiency of power conversion from 20V dc bus to notebook is 100%. In the simulated curve, the total efficiency is approaching maximum at the voltage of 20V. 20V can be used as the preferred lower dc voltage in the DC distribution system.

E. Simulation Results

Both the quality of power sources and interfaces limit the performance of DC distribution system. The bus voltage drop is mainly caused by the internal resistance of power sources and wires while the voltage spike is mainly related to the ability interfaces.

High quality power source (AC/DC converter) and power interface (DC/DC converter) should be selected to build the well performance DC distribution system. Employing energy storage device with high power/energy density can also contribute to improve the ability of anti-load-disturbance. Meanwhile, the soft-start and soft-stop techniques also should be developed to reduce the pulse impact on the DC buses.

VI. Development of DC Distribution Standards

A. Protection and Electrical Safety Standard

System protection and electrical safety facilities, which are well-established in AC power systems, but little practice exists for DC systems. The existing DC standards for protection and electrical safety standard is re-configured to set up the DC distribution standard. This standard is formulated with a view to ensuring personal and property safety, energy conservation, advanced technology, full function, economic rationality, reliable electrical installation as well as convenient installation and operation in the design of low-voltage DC distribution electrical installations. This standard is applicable to the design of low-voltage DC distribution electrical installations at 1000VDC in construction, extension and renovation engineering. The DC Distribution Standards for Protection and Electrical Safety developed mainly includes 1) Rules for Selection of DC Distribution Conductors; 2) Safety measures in arrangement of DC distribution equipment; 3) Protection of DC distribution line, etc.

B. The DC Distribution Standard for switch gear

The DC Distribution Standard for switch gear covers DC Distribution power circuit-breaker switch gear assemblies. In this standard, the ratings of a DC switchgear assembly are designations of operating limits under specified conditions of ambient temperature and temperature rise. DC Switchgear shall have the following ratings: (1) Rated maximum voltage; (2) Rated insulation level; (3) Rated continuous current; (4) Rated short-time current; (5) Rated short-circuit current Physical and electrical conditions for tests and methods of determining temperatures and test values have been established. The voltage shall be 1000 V or below.

C. Standard for retrofitting

In the past, AC is used for most of the transmission and distribution system because a simple transformer can provide the AC voltage conversion whereas DC cannot be used in transformer for voltage step-up and down. With the development of renewable energy technology, the AC energy production is replaced by DC. The conventional two-stage conversion that is the AC-DC and DC-AC for AC-AC conversion to AC appliances is not usable for DC distribution network. It is possible to skip one stage conversion and to use DC-DC conversion only by using DC for distribution systems. The developed standard for retrofitting includes retrofitting of power supplies, Inverter Air conditioner, Motor Drive & Inverter, LED Driver, Charger, Solar Power Conditioning, Wind Power Generation and Fuel Cell Power Generation. In these applications, the AC-DC stage is skipped and the main power is directly connected to the DC bus.

VII. Conclusion

DC distribution is a future technology. Today, all the necessary materials and electronics are ready to realize this new method to a city, building and office or home. It represents the high efficient, high dynamic performance and an environmentally friendly method of processing electric power. The new method will change the electricity concept and usage in all electrical parts and units. It will change the world electricity market. It is obvious to enhance the control and safety and reduce the energy loss and materials. The detailed electric and performance standard includes choice of voltage level, selection of one or two layer DC distribution structure. The analysis and simulation platform of DC systems have set up to examine the new DC distribution system. That includes steady-state and transient simulations under different operating conditions, load type, storage device and renewable energy source. Power distribution technology, switching method, protection and electrical safety, retrofitting to the electrical appliances, interfacing with the renewable energy and energy storage have been developed. A new set of standard has been developed that will be used to support the new method of DC distribution.

References

[1] S. Luo, and I. Batarseh, “A review of Distributed power systems Part 1: DC distributed power system”, *IEEE Aerosp. Electron. Syst. Mag.*, vol. 21, no. 6, Jun. 2006, pp. 5-14.

[2] S. G. Luo, I. Batarseh, “A review of distributed power systems part2: high frequency ac distributed power systems”, *IEEE A&E Mag.*, vol. 21, no. 6, June. 2006, pp. 5-13.

[3] D. Boroyevich, I. Cvetkovic, D. Dong, R. Burgos, F. Wang, F. C. Lee, “Future electronic power distribution system- a contemplative view”, OPTIM’ 2010, pp. 1369 – 1380.

[4] M. N. Marwali, A. Keyhani, “Control of distributed generation systems-part 1: voltages and current controls”, *IEEE Trans. on Power Electron.*, vol. 19, no. 6, Nov. 2004, pp. 1541-1550.

[5] M. N. Marwali, J. W. Jung, A. Keyhani, “Control of distributed generation systems-part 2: load sharing controls”, *IEEE Trans. on Power Electron.*, vol. 19 , no. 6, 2004, pp. 1551-1561.

[6] K. W. E. Cheng, “Overview of the dc power conversion and distribution”, *Asian Power Electron. J.*, Oct. 2008, vol. 2, no. 2, pp. 75-82.

[7] L. X. Tang; B. T. Ooi, “Locating and isolating dc faults in multi-terminal dc systems”, *IEEE Trans. on Power Del.*, vol. 22, no. 3, 2007, pp. 1877-1884.

[8] M. E. Baran; N. R. Mahajan, “Overcurrent protection on voltage-source-converter based multiterminal dc distribution systems”, *IEEE Trans. on Power Del.*, vol. 22, no. 1, 2007, pp. 406 – 412.

[9] E. Cinieri, A. Fumi, V. Salvatori, C. Spalvieri, “A new high-speed digital relay for the 3-kV dc electrical railway

lines", *IEEE Trans. on Power Del.*,vol. 22, no. 4, 2007, pp. 2262-2270.
[10] F. Luo; J. Chen; X. H. Lin; Y. Kang; S. X. Duan, "A novel solid state fault current limiter for dc power distribution network", APEC Conference, 2008, pp. 1284-1289.
[11] D. Salomonsson, L. Soder, A.Sannino, "Protection of low voltage dc microgrids", *IEEE Trans. on Power Del.*,vol. 24, no. 3, 2009, pp. 1045-1053.
[12] B. Morton, I. M. Y. Mareels, "The prospects for dc power distribution in buildings", AUPEC'99.
[13] H. Pang; E. Lo, B. Pong, "Dc electrical distribution systems in buildings", ICPESA '06, pp. 115-119.
[14] K. Engelen, J, Dridsen, et al., "Small-scale residential dc distribution systems", 3rd IEEE Benelux Young Reasearchers Symposium in Electrical Power Engineering, Ghent (2006-4), pp. 1-7.
[15] P. Pertti, K. Tero, P. Jarmo, "Dc supply of low voltage electricity appliances in residential buildings", CIRED' 2009, pp. 1-4.
[16] V. Sithmolada, P. W. Sauer, "Facility-level dc vs. typical ac distribution for data centers", TENCON 2010, Nov. 2010, pp. 2102-2107.
[17] Tabari, M.; Yazdani, A., "Stability of a dc Distribution System for Power System Integration of Plug-In Hybrid Electric Vehicles," *IEEE Trans. on Smart Grid* , vol.5, no.5, pp.2564,2573, Sept. 2014
[18] Wu, T.-F.; Chang, C.-H.; Lin, L.-C.; Yu, G.-R.; Chang, Y.-R., "DC-Bus Voltage Control With a Three-Phase Bidirectional Inverter for DC Distribution Systems," *IEEE Trans. on Power Electron.*, vol.28, no.4, pp.1890,1899, April 2013
[19] Mohsenian-Rad, H.; Davoudi, A., "Towards Building an Optimal Demand Response Framework for DC Distribution Networks", *IEEE Trans. on Smart Grid*, vol.5, no.5, pp.2626,2634, Sept. 2014
[20] Byeon, G.; Yoon, T.; Oh, S.; Jang, G., "Energy Management Strategy of the DC Distribution System in Buildings Using the EV Service Model", *IEEE Trans. on Power Electron.*, vol.28, no.4, pp.1544,1554, April 2013
[21] Guerrero, J.M.; Davoudi, A.; Aminifar, F.; Jatskevich, J.; Kakigano, H., "Guest Editorial: Special Section on Smart DC Distribution Systems," *IEEE Trans. on Smart Grid*, vol.5, no.5, pp.2473,2475, Sept. 2014
[22] Sato, Y.; Tanaka, Y.; Fukui, A.; Yamasaki, M.; Ohashi, H., "SiC-SIT Circuit Breakers With Controllable Interruption Voltage for 400-V DC Distribution Systems," *IEEE Trans. on Power Electron.* , vol.29, no.5, pp.2597,2605, May 2014
[23] Kazemlou, S.; Mehraeen, S., "Decentralized Discrete-Time Adaptive Neural Network Control of Interconnected DC Distribution System," *IEEE Trans. on Smart Grid* , vol.5, no.5, pp.2496,2507, Sept. 2014.
[24] Seo, G.-S.; Lee, K.-C.; Cho, B.-H., "A New DC Anti-Islanding Technique of Electrolytic Capacitor-Less Photovoltaic Interface in DC Distribution Systems," *IEEE Trans. on Power Electron.* , vol.28, no.4, pp.1632,1641, April 2013.
[25] Zhan Wang; Hui Li, "An Integrated Three-Port Bidirectional DC–DC Converter for PV Application on a DC Distribution System," *IEEE Trans. on Power Electron.*, vol.28, no.10, pp.4612,4624, Oct. 2013
[26] Tsai-Fu Wu; Chia-Ling Kuo; Kun-Han Sun; Yu-Kai Chen; Yung-Ruei Chang; Yih-Der Lee, "Integration and Operation of a Single-Phase Bidirectional Inverter With Two Buck/Boost MPPTs for DC-Distribution Applications," *IEEE Trans. on Power Electron.* , vol.28, no.11, pp.5098,5106, Nov. 2013
[27] Guest editorial - special issue on power electronics in DC distribution systems," *IEEE Trans. on Power Electron.*, vol.28, no.4, pp.1507,1508, April 2013
[28] Dong, D.; Cvetkovic, I.; Boroyevich, D.; Zhang, W.; Wang, R.; Mattavelli, P., "Grid-Interface Bidirectional Converter for Residential DC Distribution Systems—Part One: High-Density Two-Stage Topology," *IEEE Trans. on Power Electron.*, vol.28, no.4, pp.1655,1666, April 2013
[29] Shamsi, P.; Fahimi, B., "Stability Assessment of a DC Distribution Network in a Hybrid Micro-Grid Application," *IEEE Trans. on Smart Grid* , vol.5, no.5, pp.2527,2534, Sept. 2014
[30] Shadmand, M.B.; Balog, R.S.; Abu-Rub, H., "Model Predictive Control of PV Sources in a Smart DC Distribution System: Maximum Power Point Tracking and Droop Control," *IEEE Trans. on Energy Convers.*, vol.29, no.4, pp.913,921, Dec. 2014
[31] Dong, D.; Luo, F.; Zhang, X.; Boroyevich, D.; Mattavelli, P., "Grid-Interface Bidirectional Converter for Residential DC Distribution Systems—Part 2: AC and DC Interface Design With Passive Components Minimization," *IEEE Trans. on Power Electron.* , vol.28, no.4, pp.1667,1679, April 2013
[32] Kim, H-.S.; Ryu, M-.H.; Baek, J-.W.; Jung, J-.H., "High-Efficiency Isolated Bidirectional AC–DC Converter for a DC Distribution System," *IEEE Trans. on Power Electron.*, vol.28, no.4, pp.1642,1654, April 2013
[33] Kakigano, H.; Miura, Y.; Ise, T., "Distribution Voltage Control for DC Microgrids Using Fuzzy Control and Gain-Scheduling Technique," *IEEE Trans. on Power Electron.*, vol.28, no.5, pp.2246,2258, May 2013
[34] Nuutinen, P.; Pinomaa, A.; Ström, J.-P.; Kaipia, T.; Silventoinen, P., "On Common-Mode and RF EMI in a Low-Voltage DC Distribution Network," *IEEE Trans. on Smart Grid* , vol.5, no.5, pp.2583,2592, Sept. 2014
[35] Riccobono, A.; Santi, E., "Comprehensive Review of Stability Criteria for DC Power Distribution Systems," *IEEE Transactions on Ind. Appl.*, vol.50, no.5, pp.3525,3535, Sept.-Oct. 2014
[36] Fletcher, S.D.A.; Norman, P.J.; Fong, K.; Galloway, S.J.; Burt, G.M., "High-Speed Differential Protection for Smart DC Distribution Systems," *IEEE Trans. on Smart Grid* , vol.5, no.5, pp.2610,2617, Sept. 2014
[37] Hamad, A.A.; Farag, H.E.; El-Saadany, E.F., "A Novel Multiagent Control Scheme for Voltage Regulation in DC Distribution Systems," *IEEE Trans. on Sustain. Energy*, vol.6, no.2, pp.534,545, April 2015
[38] Soeiro, T.B.; Vancu, F.; Kolar, J.W., "Hybrid Active Third-Harmonic Current Injection Mains Interface Concept for DC Distribution Systems," *IEEE Trans. on Power Electron.*, vol.28, no.1, pp.7,13, Jan. 2013
[39] Chang, Y.-C.; Kuo, C.-L.; Sun, K.-H.; Li, T.-C., "Development and Operational Control of Two-String Maximum Power Point Trackers in DC Distribution Systems," *IEEE Trans. on Power Electron.* , vol.28, no.4, pp.1852,1861, April 2013
[40] Stupar, A.; Friedli, T.; Minibock, J.; Kolar, J.W., "Towards a 99% Efficient Three-Phase Buck-Type PFC Rectifier for 400-V DC Distribution Systems," *IEEE Trans. on Power Electron.* , vol.27, no.4, pp.1732,1744, April 2012
[41] Gab-Su Seo; Jong-Won Shin; Bo-Hyung Cho; Kyu-Chan Lee, "Digitally Controlled Current Sensorless Photovoltaic Micro-Converter for DC Distribution," *IEEE Trans. on Ind. Inform.*, vol.10, no.1, pp.117,126, Feb. 2014.
[42] IEC 479-1: 1994 Guide to Effects of current on human beings and livestock

ACKNOWLEDGMENT

The author grateful acknowledge the financial support of the Hong Kong Innovation and Technology Fund University-Industry Collaboration Programme under the

project reference (UIM/245) and the support from the sponsor.

BIOGRAPHIES

K. Ding received the B.E., M.E., and Ph.D. degrees from Huazhong University of Science and Technology, Wuhan, China, in 1998, 2001, and 2004, respectively. He is currently a Research Fellow with the Power Electronics Research Centre, Department of Electrical Engineering, Hong Kong Polytechnic University, Kowloon, Hong Kong. His research interests include multilevel converters, Solar auto-tracking system, fuel cell techniques, electrical vehicles, Distributed Power Generation System, battery-management systems, Polymer-bonded Magnetic , Integrated Battery charger and motor Drive System, dynamic voltage restorers, power electronics applications in electric power systems, and computer simulation.

K.W.E.Cheng obtained his BSc and PhD degrees both from the University of Bath in 1987 and 1990 respectively. Before he joined the Hong Kong Polytechnic University in 1997, he was with Lucas Aerospace, United Kingdom as a Principal Engineer.
He received the IEE Sebastian Z De Ferranti Premium Award (1995), outstanding consultancy award (2000), Faculty Merit award for best teaching (2003) from the University, Faculty Engineering Industrial and Engineering Services Grant Achievement Award (2006) and Brussels Innova Energy Gold medal with Mention (2007), Consumer Product Design Award (2008), Electric vehicle team merit award of the Faculty (2009), Special Prize and Silver Medal of Geneva's Invention Expo (2011) and EcoStar Award (2012). He has published over 250 papers and 7 books. He has over 100 interviews by media on his research and development. He is now the professor and director of Power Electronics Research Centre of the university.

D.H. Wang obtained his bachelor degree in Industrial Automation department from Jiangxi University of Science and Technology, Ganzhou, China, in 2000. He received his master degree in power electronics and drives department from Shanghai University, Shanghai, China, in 2003. Currently, he is a research associate in the department of Electrical Engineering at the Hong Kong Polytechnic University, Hong Kong. His research interests include busbars, power electronics, motor drive, lighting control, new energy management, power quality control.

Y.M. Ye received the B.Sc. degree in electrical engineering from University of Jinan, Jinan, China, in 2007, and the M.Sc. degree in control theory and control engineering from South China University of Technology, Guangzhou, China, in 2010. He is currently working toward the Ph.D. degree with the Department of Electrical Engineering, Faculty of Engineering, Hong Kong Polytechnic University, Hong Kong. From September 2010 to January 2014, he was with the Department of Electrical Engineering, Faculty of Engineering, Hong Kong Polytechnic University, as a Research Assistant. His research interests include various dc-dc power converters, switched-capacitor technique and its applications, multilevel inverters, power conversion and energy management for smart-grids, protection and control techniques for DC distribution.

X.L. Wang obtained her bachelor degree in Electrical Engineering and Automation from Three Gorges University, Yi Chang, China, in 2012. She received her master degree in Electrical Engineering from the Hong Kong Polytechnic University, Hong Kong, in 2013. Currently, she is a Ph.D. student in the department of Electrical Engineering at the Hong Kong Polytechnic University, Hong Kong.

J.F.Liu received the M.S. degree in control engineering from the South China University of Technology, Guangzhou, China, in 2005, and the Ph.D. degree from the Hong Kong Polytechnic University, Kowloon, Hong Kong,in 2013. From 2005 to 2008, he was a development engineer of Guangdong Nortel Network, Guangzhou, China. Currently, he was a Research Associate at Electrical Engineering Department of Hongkong Polytechnic Uiniversity. His research interests include power electronics applications, nonlinear control, and high frequency power distribution system.

Author Index

Submission details

Only online submission will be accepted. Please first register and submit online. The paper is in double column and is similar to most IET or IEEE journal format. There is no page limit. Any number of pages of more than 6 will be subject to additional charge.

The paper guidelines can be downloaded using the link: http://perc.polyu.edu.hk/apejournal/

Any queries, please contact Prof. Eric Cheng, Publishing Director of APEJ, Dept. of Electrical Engineering, The Hong Kong Polytechnic University, Hung Hom, Hong Kong. Email: eeecheng@polyu.edu.hk Fax: +852-2330 1544

Any secretarial support and production related matters, please contact Dr. James Ho, Power Electronics Research Centre, The Hong Kong Polytechnic University, Hung Hom, Hong Kong. Email: eeapej@polyu.edu.hk Tel: +852-3400 3348 Fax: +852-3400 3343

Publication Details

The Journal will be published 2-3 times a year. The first issue was published in 2007. Response time for paper acceptance is within 3 months. The APEJ is an open access journal that is available to the reader to have free downloaded electronically.

Financial Charge

All the accepted papers will be printed without charge for 6 or less pages. An additional page charge is HK$100 per page. A hardcopy of the journal will be posted to the corresponding author free of charge. Additional copies of the journal can be purchased at HK$200 each. The charge includes postage and packing.

All Chinese Papers will be subjected to a translational fee of HK$350 per page. It will be charged when the paper is accepted for publication.

Advertising

Advertisement is welcome. Full page advertisement is HK$1000. For colour advertisement, the amount is doubled. All the advertisement will be both posted online in the journal website and hardcopy of the journal.

For advertising enquiries and details, please contact eeapej@polyu.edu.hk . Tel: +852-3400 3348 Fax: +852-3400 3343

For payment, please send your cheque, payable to ‘The Hong Kong Polytechnic University, address to Ms. Kit Chan, Secretary of APEJ, Dept. of Electrical Engineering, The Hong Kong Polytechnic University, Hung Hom, Hong Kong.